THE ASTROPHYSICAL JOURNAL, 434:570–586, 1994 October 20

GENERALIZED COMPTONIZATION MODELS AND APPLICATION TO THE RECENT HIGH-ENERGY OBSERVATIONS

LEV TITARCHUK[1]
Laboratory for High Energy Astrophysics, NASA/GSFC, Greenbelt, MD 20771
Received 1993 September 23; accepted 1994 April 26

ABSTRACT

The theory of spectral formation in thermal X-ray sources, where the effects of Comptonization and Klein–Nishina corrections are important, is presented. Analytical expressions are obtained for the produced spectrum as a function of such input parameters as the plasma temperature, the optical depth of the plasma cloud and the injected soft photon spectrum. The analytical theory developed here takes into account the dependence of the scattering opacity on the photon energy. It is shown that the plasma temperature as well as the asymptotic rate of photon escape from the plasma cloud determine the shape of the upscattered hard tail in the emergent spectra, even in the case of very small optical depths. The escape distributions of photons are given for any optical depth of the plasma cloud and their asymptotic dependence for very small and large optical depths are examined. It is shown that this new generalized approach can fit spectra for a large variety of hard X-ray sources and determine the plasma temperature in the region of main energy release in Cyg X-1 and the Seyfert galaxy NGC 4151.

Subject headings: gamma rays: theory — plasmas — radiation mechanisms: nonthermal — X-rays: stars

1. INTRODUCTION AND SUMMARY

Three radiation processes have been found to be of prime importance in hot plasmas: bremsstrahlung, synchrotron (cyclotron) radiation, and Compton scattering; in compact enough plasmas, they are complemented by pair production and annihilation. During recent years it has become clear that the proper interpretation of the spectra of gamma-ray sources as well as of the underlying physical processes is impossible without the detailed accounting for Compton scattering. The latter occurs in a variety of forms (thermal and nonthermal, upscattering and downscattering) and includes such process as inverse Compton scattering, Comptonization, reflection, backscattering, etc. For a review of these topics and some implications, see Brinkmann, Fabian, & Giovanelli (1990) and Zdziarski et al. (1993b), where references to earlier work are also given. The shape of the radiation spectra generated by Comptonization in a plasma cloud of finite optical depth was the subject of our previous papers (Sunyaev & Titarchuk 1980, 1985, 1989; Titarchuk 1987, 1988).

The main motivation that forced us to return to the problem of Comptonization is a number of fine recent measurements of the radiation spectra of the X-ray emitting AGN (Apal'kov et al. 1992; Maisack et al. 1993; Yaqoob et al. 1993) and Cyg X-1 (Salotti et al. 1992; Grabelsky et al. 1993).

The observed spectra agree well with analytically derived radiation spectra due to Comptonization of low-frequency photons in isothermal plasma. The previous measurements of Cyg X-1 showed that the plasma temperature in the cloud is $kT_e \simeq 26.5$ keV and the optical depth of its disk with respect to the electron scattering is $\tau_0 \simeq 4$ (Sunyaev & Trümper 1979; Sunyaev & Titarchuk 1980). An attempt to interpret the recent observations of Cyg X-1 and NGC 4151 yield smaller optical depths ($\tau_0 < 1$ for Cyg X-1, and $\tau_0 \sim 3$ for NGC 4151) and much higher plasma temperatures $kT_e > 50$ to 150 keV. At high temperatures, the effectiveness of the Comptonization process increases substantially. As a result even at moderate τ_0 one has a Comptonization parameter

$$y \sim \frac{4kT_e}{m_e c^2}\,\tau_0^2 \gg 1 .$$

Therefore, in order to explain the observed spectra, whose overall shape is far from Wien, one concludes that $\tau_0 < 1$ (e.g., Cyg X-1). In this case the validity of nonrelativistic Comptonization theory, (Sunyaev & Titarchuk 1980, hereafter ST80) in the diffusion approximation is under some question. Thus spectral formation from disks or plasma cloud of comparatively small optical depth at the high plasma temperatures should be examined.

The present paper deals in detail with the following points: (a) the general formulation of the Comptonization radiative transfer problem and its reduction to the diffusion problem over energy and space; (b) the time dependence of photon escape from disk and spherical geometries; (c) the shape of the radiation spectra, taking into account relativistic corrections in the free electron cross section and the scattering kernel; (d) the source of low-frequency photons; and (e) the recent high-energy observations and their possible interpretation by thermal Comptonization models.

Comptonization is the problem of energy exchange in the scattering of photons off electrons. The average energy exchange per scattering is determined by the relation between the photon and electron energies. For a thermal electron distribution with temperature kT_e and nonrelativistic electron energies $h\nu$, ($h\nu$. $kT_e \ll m_e c^2$), we have as follows:

$$\frac{\langle \Delta\nu \rangle}{\nu} = \frac{4kT_e - h\nu}{m_e c^2} .$$

When the photon energy $h\nu$ is much less than the mean electron energy kT_e, the photon gains energy due to the Doppler effect, i.e.,

$$\frac{\langle \Delta\nu \rangle}{\nu} = \frac{4kT_e}{m_e c^2} .$$

[1] NAS/NRC Senior Research Associate.

In the opposite case, ($h\nu \gg kT_e$), the photon loses its energy because of the recoil effect.

In a finite medium (plasma cloud) two processes compete with each other, and influence the formation of emergent spectra: photon diffusion over space, and photon diffusion over energy. The photons gain or lose energies in a random walk around the plasma cloud. The Comptonization parameter

$$y_{\rm tr} = \frac{4kT_e}{m_e c^2} c\sigma_{\rm T} n_e t$$

determines the photon energy gain due to the Doppler effect along a random trajectory with time duration t. Here n_e is the electron density and $\sigma_{\rm T}$ is the Thomson cross section. The photon distribution over the random walk time is controlled by the plasma cloud boundary conditions (photons are not scattered out of plasma cloud, see eq. [A8]). For a plasma cloud with optical depth $\tau_0 \gg 1$, the mean number of scatterings $\bar{u} \sim \tau_0^2$ and thus the mean Comptonization parameter

$$y \sim \frac{4kT_e}{m_e c^2} \tau_0^2 .$$

The most important case is when unsaturated Comptonization spectra are formed (ST80), $3 < y < 12$ [$1 < \gamma \simeq (12/y) < 4$]. The primary low-frequency photons with mean energy, $h\nu_0$ ($h\nu_0 \ll kT_e$) are distributed through the plasma cloud. Some of them which suffer a number of scatterings u much less than the average $\bar{u}$, retain information about the initial spectral, angular and space distribution. In principle, we can restore this information by analyzing the observed X-ray spectrum. But the photons which undergo a number of scatterings u much greater than the average $\bar{u}$, form specific spectral and angular distributions which are mainly characterized by the plasma cloud optical depth τ_0 and temperature kT_e, and which are almost independent of the initial distribution of the low-frequency photons (Sunyaev & Titarchuk 1985, hereafter ST85).

For higher values of y, the Wien spectrum is established as a result of the equilibrium between photons and electrons, and therefore, this case is trivial.

In order to solve the Comptonization problem we should distinguish two regions: (I) When the plasma cloud optical depth τ_0 is greater than 1 and (II) When τ_0 is less than 1.

The first case is treated in §§ 2 and 3.1. The radiative problem is reduced to the diffusion problem in energy space and configuration space. For example, the drift of photons along the vertical coordinate,

$$H = \frac{\tau_0}{\sigma_{\rm T} N_e} ,$$

gives rise to the photon trajectory length $l = H\tau_0$, τ_0 times more than the vertical drift. Also, since there is no preferential direction for photon propagation in a plasma cloud, the radiation field is almost isotropic. The radiative transfer equation for the intensity along a certain direction is replaced by the equation for the intensity averaged over all photon directions. The integral collision term of the radiative transfer equation, along with the loss term, are transformed into the energy diffusion term. The intensity space gradient term is transformed into the diffusion space term for the average intensity, (see details of the reduction of the radiative transfer to the diffusion problem in Appendix A). Finally, the emergent spectrum of X-ray radiation is obtained as a convolution of two functions: One is the diffusion solution for the time evolution of the initial low-frequency photon spectrum in the infinite medium (the Cauchy problem solution) which was found by Kompaneets (1956) for the nonrelativistic case ($h\nu \ll m_e c^2$), and the second is the photon distribution over the escape time $u = \sigma_{\rm T} n_e ct$ (proof of this statement appears in § 2.1 and Appendix A). In other words, the distribution determines the probability that the photon escapes from the plasma cloud in the interval u to $u + 1$. This is a well-known problem solved elsewhere (e.g., ST80; ST85).

In order to generalize the Comptonization problem for the case of subrelativistic energies and plasma temperatures, we should take into account the relativistic corrections introduced into the diffusion coefficients of the energy and space operators (Prasad et al. 1988; Shestakov, Kershaw, & Prasad 1988; § 2.1 and Appendix A, B in this paper). The diffusion coefficient of the energy operator η_ν is obtained by weighting the energy shift with the Compton Scattering Kernel (CSK) (Prasad et al. 1988). The CSK is a result of integrating the Klein–Nishina cross section for Compton scattering of an electron over a relativistic Maxwellian distribution of electrons (Pomraning 1973). The inclusion of the relativistic corrections increases η_ν when the plasma temperature goes up. The corrected coefficient contains the additional temperature dependent factor $f = 1 + 2.5\Theta + \cdots$ (e.g., Prasad et al. 1988). Here Θ is a dimensionless temperature normalized with respect to the electron rest energy

$$\Theta = \frac{kT}{m_e c^2} .$$

In the very hard tail ($h\nu > 200$ keV), photons are mainly scattered in the forward direction and change their energy only slightly. The Compton effect loses effectiveness, and hence the coefficient η_ν drops.

The diffusion coefficient in the space operator φ_ν is obtained by averaging the cosine square of the angular variable ϑ over all photon directions. As an example, this equals to $\frac{1}{3}$ for an isotropic radiation field. This approximation is valid for nonrelativistic energies and temperatures. However, in the course of a random walk, photons are getting harder because of upscattering, the Klein–Nishina differential cross section strongly deviates from the Rayleigh one, and the approximation of isotropic radiation field breaks down. The space diffusion coefficient is corrected by the transport factor $\lambda_{\rm tr}$ which takes into account the scattering anisotropy (Grebenev & Sunyaev 1988; Shestakov et al. 1988). In particular, for subrelativistic energies and temperatures, Shestakov et al. (1988) derive the asymptotic behavior of $\lambda_{\rm tr}$ as follows:

$$\lambda_{\rm tr}^{-1} = 1 - \tfrac{16}{5} z + 2\Theta + \cdots < 1 ,$$

where $z = h\nu/m_e c^2$.

We give here a short description of changes in the emergent spectral shape caused by the relativistic corrections.

At small energies ($h\nu < kT_e$) the spectrum becomes harder, i.e., the spectral index drops as a result of the growth of the energy diffusion coefficient η_ν. Also, the hard energy tail ($h\nu > kT_e$) is steeper than what we have in the nonrelativistic case, since all scattering processes in energy and space are suppressed—the coefficient η_ν decreases, and the coefficient $\varphi_\nu = \lambda_{\rm tr}/3$ increases along the photon energy axis. In § 2.1 and

Appendix A, we give the derivation of the Fokker–Plank equation. It is the solution of this equation which determines the emergent spectrum.

The next points should be emphasized: (i) Photons undergoing many more scatterings, $u = \sigma_T n_e ct$ than the mean value, $\bar{u}$ escape from the plasma cloud in accordance with the exponential law, i.e., the asymptotic distribution over escape time $P_{as}(u) \propto \exp(-\beta u)$. The final spectral shape in the upscattering case is determined by these photons only. Therefore, instead of deriving the full solution which is too complicated, we find the upscattering asymptotic solution of the Comptonization Stationary Equation (this is obtained from the Fokker–Plank equation (9) and equation (10) through a Laplace transformation with the parameter β, (eqs. [15] and [29]). (ii) The shape of the emergent spectrum is calculated numerically and analytically by solving equation (15). For the numerical solution we use the Run method for the conversion of the three diagonal matrix operator. The analytical solution combines some modification of our previous spectrum, ST80 and new relativistic hard tail in the form $F_\nu \propto x^{3-b_1} e^{-x(1+b_0)}$ (for details see § 3.1).

In §§ 2.1 and 3.2 we discuss the second problem of upscattering in the small optical depth case. Even in this case the X-ray spectrum is created by photons which suffer many more scatterings in plasma cloud than the average number (ST80; ST85). However these photons produce the specific radiation field, with the specific angular and space distributions which are only determined by the plasma cloud optical depth and are independent of energy (ST85), i.e., photon random walk around plasma cloud occur independently on photon energy change (gain). Thus the upscattering spectral formation in the case of small optical depths can also be considered in terms of the Fokker–Plank approach when the photon energy change is weighted by the Compton scattering kernel (CSK) over photon directions and the photon scattering distribution. All previous calculations of the diffusion coefficients (e.g., Prasad et al. 1988) are obtained for isotropic radiation field distribution and therefore they are not valid in our case. The structure of the radiation field created by photons which undergo repeated scattering is quite different from isotropic. Most photons are collimated along the longest size of the plasma cloud (in spherical geometry this is along a diameter; in disk geometry it is along the disk). Therefore, we can simplify the radiative transfer problem by considering only scatterings along the forward and backward directions. However photon scatterings off electrons in the forward direction does not produce any change of in the photon energy. Only backward scatterings change the photon energy. When the plasma temperature grows, the Klein–Nishina phase function becomes sharper along the forward direction, and consequently, the backward part is more suppressed. As a result, Compton scattering is not so efficient in the collimated field as it is in the isotropic field, and hence, the temperature amplification factor of the energy diffusion coefficient η_ν is weaker in the former case than the latter one. The ratio of two factors is

$$\frac{f_{col}}{f_{iso}} = \frac{1 + (19/8)\Theta \ldots}{1 + (35/8)\Theta \ldots}.$$

Here, f_{col} and f_{iso} are the temperature factors of the energy diffusion coefficient η_ν in the collimated and isotropic cases respectively. This difference of the temperature dependences changes dramatically the power law spectral slope estimates. For example, for the spherical plasma cloud case with optical depth $\tau_0 = 0.5$ and $kT_e = 250$ keV, we get the power law spectral slope $\alpha_{col} = 0.60$ instead of the isotropic value $\alpha_{iso} = 0.43$. The Monte Carlo calculations (Titarchuk & Hua 1994; Pozdnyakov, Sobol, & Sunyaev 1983; Zdziarski 1986) confirm our Fokker–Plank approach of the Comptonization problem for the optically thin case.

Self-consistent hydrodynamic equilibrium calculations result, in a number of cases, in a nonisothermal temperature distribution. The simplest realization of such nonisothermality is the sandwich model (Sunyaev & Titarchuk 1989; Haardt & Maraschi 1991): A cold layer produces low-frequency photons which are subject of Comptonization in hot layer (there is no lack of mechanism to heat that layer, see e.g., Guessoum & Kazanas 1990). If the temperature distribution of the hot plasma is more or less homogeneous, the resulting spectrum can be described by some mean temperature (Titarchuk 1988). Section 4 refers to the sandwich model. We derive there the equation for the self-consistent determination of the low-frequency photon energy. The astrophysical applications of the developed theory to recent high-energy observations are shown in § 5. A full survey of the conclusions is given in § 6.

2. RADIATIVE TRANSFER THEORY

2.1. *Basic Equations*

The photons which undergo, on average, many more than one scattering, independent of the optical depth of the plasma cloud, produce the typical diffusion field of radiation and can be described by the diffusion (Fokker–Plank) approximation (see for details Appendix A and Shestakov et al. 1988). In this section we consider the case with the plasma cloud optical depth $\tau_0 \gg 1$ and we present all calculations of the appropriate diffusion coefficients. The diffusion coefficients are obtained as a result of averaging over all solid angles which is relevant only in the large optical depth case. The transport scattering cross section used in the coefficient of the spatial diffusion is $D = c/3\sigma_{tr} n_e$ takes into account that fact that small angle scatterings weakly change the photon trajectories. The transport cross section of scattering by electrons is given by

$$\sigma_{tr} = \frac{\sigma_T}{\lambda_{tr}(\nu, \Theta)} = \int \left(1 - \frac{\nu}{\nu'} \cos \vartheta\right) d\sigma_c(\nu \to \nu'), \quad (1)$$

where $d\sigma_c(\nu \to \nu')$ is the differential cross section of Compton scattering averaged over the Maxwellian distribution (e.g., Pomraning 1973; Shestakov et al. 1988), ν and ν' are the frequencies of photons before and after the scattering, ϑ is the scattering angle, σ_T is Thomson cross section and

$$\Theta = \frac{kT_e}{m_e c^2}$$

is the dimensionless plasma temperature.

The factor λ_{tr} can be written with an accuracy of better than 2% in the range $h\nu < 1$ MeV for $\Theta = 0$, by the formula (Grebenev & Sunyaev 1987)

$$\lambda^0_{tr}(z) = 1 + 2.8z - 0.44z^2, \quad (2)$$

where $z = (h\nu/m_e c^2)$. It is worthwhile to point out that λ_{tr} is also a weak function of temperature (see Fig. 2 in Shestakov et al. 1988), and we can take into this dependence as follows

$$\lambda_{tr}(z) = [1 + 2.8(1 - 1.1\Theta)z - 0.44z^2]. \quad (2a)$$

The time evolution of the photon energy is determined by the Doppler and recoil effects through the energy diffusion coefficent $\eta(z, \Theta)$ which is found by solving the differential

equation (Prasad et al. 1988).

$$\eta - \Theta \frac{\partial \eta}{\partial z} = \langle (z - z') \rangle = \int_0^\infty (z' - z) dS_c(z \to z', \Theta) . \quad (3)$$

Here $S_c(z \to z', \Theta)$ is the scattering kernel of the Compton kinetic equation (e.g., Pomraning 1973; Shestakov et al. 1988). The exact analytical formula for the diffusion coefficient $\eta(z, \Theta)$ was derived by Prasad et al. (1988). But with accuracy 1% in the range $kT_e < 100$ keV, $\eta(z, \Theta)$ may be approximated by the formula (see Cooper 1971)

$$\eta(z, \Theta) = \frac{z^4}{1 + 4.6z + 1.1z^2} \left[1 + \frac{f_0(\Theta)}{1 + 10.2z} \right], \quad (4)$$

Here $f(\Theta)$ is

$$f_0(\Theta) = 2.5\Theta + 1.875\Theta^2(1 - \Theta) . \quad (5)$$

In the diffusion (i.e., Fokker–Plank) approximation ($\tau_0 \gg 1$) the problem of radiative transfer can be reduced to the solution of the differential equation (see the proof of this statement in Appendix A, eqs. [A6] and [A8])

$$L_\nu n + L_\tau^{(d)} n = - \frac{B_0(x, \tau) \lambda_{tr}^{-1}(x\Theta)}{x^3} \quad (6)$$

with appropriate boundary conditions (see Appendix A, eq. [A8] and also ST80; ST85; Grebenev & Sunyaev 1987).

Here

$$L_\nu = \frac{\Theta \lambda_{tr}^{-1}(x\Theta)}{x^2} \frac{\partial}{\partial x} \left[\eta(x\Theta, \Theta) \left(\frac{\partial}{\partial x} + E \right) \right], \quad (7)$$

and space operators L_τ^d for spherical and plane geometries are presented by equations (20) and (A9) respectively. Equation (6) is written using the dimensionless variables $\tau = \tau_T$ and $x = h\nu/kT_e$; $n(x, \tau) = I_\nu c^2/2\nu^3$ is the photon occupation number in phase space and $B_0(x, \tau)$ is the primary source distribution.

The first term of the left-hand side of the equation (6) describes the photon dispersion and shift due to Doppler and recoil effects on electrons. The second relates to spatial diffusion.

If we suppose that this term

$$\Phi(\tau, x) = \frac{B_0(x, \tau) \lambda_{tr}^{-1}(x\Theta)}{x^3} = \psi(x) r(\tau) ,$$

i.e., is factorable into functions of x and τ alone (in fact any such term is expended in series over the eigenfunctions of the space operator L_τ) then it is easy to prove that the solution of equation (6) can be represented by the following convolution (see the proof in Appendix A):

$$n(x, \tau) = \int_0^\infty N(x, u) R(\tau, u) du . \quad (8)$$

$N(x, u)$ is the solution of the time-dependent problem for the energy space with $x > 0$:

$$\frac{\partial N}{\partial u} = L_\nu N , \quad (9)$$

having as initial condition

$$N(x, 0) = \psi(x) . \quad (10)$$

On the other hand, $R(\tau, u)$ is the solution of the time-dependent problem in configuration space $0 \le \tau \le 2\tau_0$ for a disk and in $0 \le \tau \le \tau_0$ for a spherical plasma cloud given by

$$\frac{\partial R}{\partial u} = L_\tau^{(d)} R \quad (11)$$

with the initial condition

$$R(\tau, 0) = r(\tau) \quad (12)$$

and with the proper boundary condition in configuration space. (e.g., Appendix A, eq. [A8]).

If $r(\tau)$ equals the first eigenfunction of the space operator L_τ^d, which is the case of interest for Compton upscattering the solution of equations (11) and (12) can then be written

$$R(\tau, u) = R_1(\tau) \exp(-\beta u) . \quad (13)$$

The main solution $n(x, \tau)$ of equation (6) is then in the very simple form

$$n(x, \tau) = n_1(x, \tau) = R_1(\tau) \int_0^\infty N(x, u) e^{-\beta u} du = R_1(\tau) N_1(x) . \quad (14)$$

In the general case the solution of the equation (6) is presented by series of the form presented in equation (14) corresponding to the different eigenfunctions L_τ^d, but the main fraction in this series is determined by the first term, $n_1(x, \tau)$, if the photons of the primary sources $B_0(x, \tau)$ have low energies ($h\nu \ll kT_e$).

The Comptonization problem for this case reduces to solving the Comptonization stationary equation (CSE) for $N_1(x)$ (compare with Chapline & Stevens 1973; Shapiro, Lightman, & Eardley 1976; ST80) given by

$$L_\nu N_1 - \beta N_1 = -\psi(x) . \quad (15)$$

In fact the above equation results from a Laplace transformation of the time-dependent problem (9) and (10).

The meaning of the convolutions in equations (8) and (14) is that the process of photon energy gain and the process of the photon random walking of photon through the plasma cloud should be considered independently. Similarly, we show in Appendix A this is also valid for photons in plasma clouds of arbitrary optical depth. The fact is that the X-ray spectrum is created by photons which suffer many more scatterings in plasma cloud than the average number (ST80; ST85). However, these photons produce the specific radiation field, with the specific angular and space distributions which are only determined by the plasma cloud optical depth and are independent of energy (ST85), i.e., photon random walk around plasma cloud occur independently on photon energy change (gain). Thus the upscattering spectral formation in the case of small optical depths can also be considered in terms of the Fokker–Plank approach when the photon energy change is weighted by the Compton scattering kernel (CSK) over photon directions and the photon scattering distribution.

In the general case, the asymptotic behavior of the photon distribution over the escape time is also described by an exponential law, $\exp(-\beta u)$ (see below eq. [17]). Hence we find that equation (15) would be valid even for small optical depth of the plasma cloud but with the appropriate correction of the diffusion coefficient η_ν for this case (see § 3.2 and Appendix A, B).

The second term of equation (15) which takes into account the spatial escape rate of photons from the plasma cloud, is proportional to the occupation number N_1 with the coefficient β. It implies that the fractional number of photons which

random walk out of the plasma cloud becomes $e^{-\beta}$ less with each collision. On the other hand we know that this number is equal to the first eigenvalue p_1 of the space scattering operator $\hat{L}$ (see eqs. [25] and [26]), i.e., thus

$$\beta = \ln(1/p_1) . \tag{16}$$

Actually, the primary source space distribution $B_0(\tau)$ is expanded in the generalized Fourier series over the eigenfunctions $\{g_i(\tau)\}$ of the scattering operator $\hat{L}$

$$B_0(\tau) = \sum_{i=1}^{\infty} a_i g_i .$$

Using the iterative method of successive approximation we obtain the term v_k responsible for photons which have undergone k-scatterings in the plasma cloud

$$v_k(\tau) = \hat{L}_\tau^k B_0 = \sum_{i=1}^{\infty} a_i p_i^k g_i .$$

Because of the sequence of the eigenvalues $\{p_i\}$ is in decreasing order (it monotonically converges to zero), i.e., $p_1 > p_2 > \cdots > p_i \to 0$ when $i \to 0$ we get that with increasing k the first term is dominant in v_k, that is

$$v_k(\tau) \simeq a_1 p_1^k g_1(\tau) .$$

It is worthwhile noting that relationship (16) is valid for any optical depth of the plasma cloud and reduces to $\beta = 1 - p_1 \propto \tau_0^{-2}$ only in the diffusion case because of $(1 - p_1) \propto \tau_0^{-2} \ll 1$. In the optically thin case $p_1 \propto \tau_0$ and thus $\beta \sim \ln(1/\tau_0)$.

The solution $N_1(x)$ determines the shape of the output spectrum which is the same throughout the plasma cloud. Generalizing the above statement one can say that for an isothermal (or with a smoothly distributed temperature) disk, the shape of the hard radiation spectrum does not depend on the low frequency photon source distribution, and it is the same at any point inside the disk (independent of the τ-coordinate) (ST85 and Titarchuk 1988).

2.2. *Distribution Law of the Number Scattering*

As we display, the problem of the X-ray spectral formation in a hot plasma cloud is closely connected with the distribution law of the number of scatterings. It is important to note that the time-dependent function $R(\tau_0\, u)$, in equations (11) and (12) determines the distribution of photons over the dimensionless time u they spend in a plasma cloud (scattering number).

The exponential tail of the distribution over the scattering number is a typical feature of the problem of photon escape from a limited region of space. This asymptotic behavior takes place in plasma cloud with arbitrary density distribution and source distribution (ST80). The probability that a photon undergoes u scatterings where $u \gg \bar{u}$ (where $\bar{u}$ is the average number of photon scattering), is given by the asymptotic relation:

$$P_{as}(u) = A(\bar{u}, \tau_0) \exp(-\beta u) , \tag{17}$$

where the normalization constant $A(\bar{u}, \tau_0)$ depends on the distribution of low-frequency photon sources, $B_0(\tau)$, inside the plasma cloud (ST80; ST85). In the diffusion approximation (applicable to the case where the optical half-thickness of the disk, τ_0, is much greater than 1), the parameter β is given by the relation $\beta = \lambda_1^2/3$ and represents the first eigenvalue of the differential operator $L_\tau^{(d)} = \frac{1}{3}(d^2/d\tau^2)$, when the boundary conditions appropriately describe photon escape from the disk. It is easy to show (see, e.g., ST85) that λ_1 is the solution of the transcendental equation:

$$\tan \lambda\tau_0 = \frac{3}{2\lambda} . \tag{18}$$

When $\tau_0 \gg 1$ this equation has the asymptotic solution

$$\lambda_1 = \frac{\pi}{2(\tau_0 + 2/3)} ,$$

and therefore:

$$\beta = \frac{\pi^2}{12(\tau_0 + 2/3)^2} \quad \text{for a disk} . \tag{19}$$

The appropriate diffusion operator in the case of a spherical homogeneous plasma cloud reads

$$L_\tau^{(d)} = \frac{1}{3}\frac{1}{\tau^2}\frac{\partial}{\partial\tau}\tau^2\frac{\partial}{\partial\tau} , \tag{20}$$

and its eigenvalues are determined by (see ST80)

$$\tan \lambda\tau_0 = \frac{\lambda\tau_0}{1 - (3/2)\tau_0} . \tag{21}$$

Here τ_0 characterizes the optical radius of the spherical cloud. The asymptotic solution of this equation, for $\tau_0 \gg 1$, is $\lambda_1 = \pi/(\tau_0 + \frac{2}{3})$, and so

$$\beta = \frac{\pi^2}{3(\tau_0 + 2/3)^2} \quad \text{for a sphere} . \tag{22}$$

In order to generalize this photon diffusion approach for the case of arbitrary optical depth τ_0, we replace the diffusion operators $L_\tau^{(d)}$ with the radiative transfer operators L_τ (see Appendix A and Chandrasekhar 1960) describing photon scattering in the plasma cloud of arbitrary optical depth. For the disk (plane) geometry this operator is

$$L_\tau = \tfrac{1}{2}\int_0^{2\tau_0} d\tau' E_1(|\tau - \tau'|) - \boldsymbol{E} = \hat{L}_\tau - \boldsymbol{E} , \tag{23}$$

while for spherical geometry it is given by

$$L_\tau = \tfrac{1}{2}\int_0^{\tau_0} d\tau'\tau'[E_1(|\tau - \tau'|) - E_1(\tau + \tau')] - \tau\boldsymbol{E} = \hat{L}_\tau - \tau E . \tag{24}$$

Here $\boldsymbol{E}$ is the identity operator and $E_1(z)$ is the exponential integral of the first order. Both diffusion operators are derived from equations (23) and (24) under the assumption of $\tau_0 \gg 1$.

The space radiative transfer equations for the source function $B(\tau)$ are written by means of operator L_τ in the following form:

$$B(\tau) = \hat{L}_\tau B(\tau') + B_0(\tau) \quad \text{for a disk} , \tag{25}$$

$$\tau B(\tau) = \hat{L}_\tau[\tau' B(\tau')] + \tau B_0(\tau) \quad \text{for a sphere} . \tag{26}$$

The solution of equations (25) and (26), obtained by successive approximations over scattering events produced the distribution laws of the number of scatterings, $P(u)$, and the asymptotic escape dimensionless rates $1/\beta$ (see, e.g., ST85).

The β values which were presented in Table 1 and Figure 2 of ST85 are given for the sake of completeness in Figure 1 here. These values are practically for any optical depth for disk and

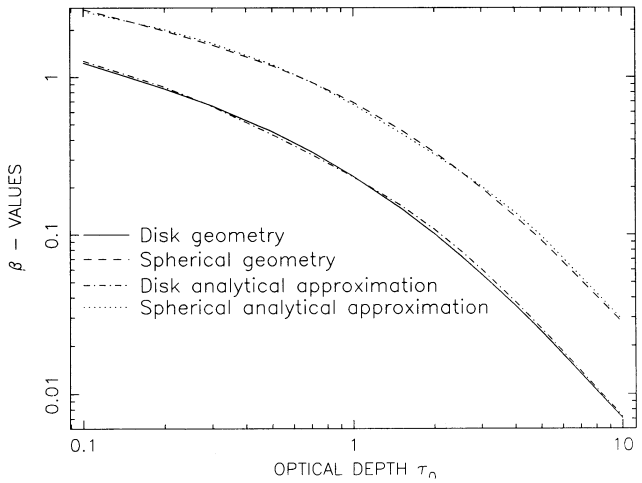

FIG. 1.—β-dependence as a function optical depth for disk geometry (*solid line*) and spherical geometry (*dashed line*). The analytical approximation β-dependence eqs. (27) and (28) are displayed by the dash-dotted curve (disk) and the dotted curve (sphere).

spherical geometries. As it can be seen, by comparing equations (19) and (22) to the results presented in Figure 1, for $\tau_0 > 3$ or 4 the diffusion approximation gives β with a satisfactory degree of accuracy. ST85 (see also eqs. [27] and [28]) presents analytical expression for the exponential law for case of small optical depth, i.e.,

$$\beta = \ln\left[\frac{2}{3\tau_0 \ln(1/2\tau_0)}\right] \quad \text{for a disk}, \tag{19a}$$

and

$$\beta = \ln\frac{4}{3\tau_0} \quad \text{for a sphere}. \tag{22a}$$

All these analytical estimates are in excellent agreement with computational results (see Table 1 of ST85). In order to present these computational calculations in an analytical form we derive the next approximations of β, which incorporate asymptotic expression for both small (eqs. [19a] and [22a]) and large (eqs. [19] and [22]) optical depths,

$$\beta = \frac{\pi^2}{12(\tau_0 + 2/3)^2}(1 - e^{-1.35\tau_0}) + 0.45e^{-3.7\tau_0}\ln\frac{10}{3\tau_0} \quad \text{for a disk}, \tag{27}$$

$$\beta = \frac{\pi^2}{3(\tau_0 + 2/3)^2}(1 - e^{-0.7\tau_0}) + e^{-1.4\tau_0}\ln\frac{4}{3\tau_0} \quad \text{for a sphere}. \tag{28}$$

The results of comparison between analytical and computational results of β are given in Figure 1.

It is worthwhile noting, that the forms of the diffusion operators $L_\tau^{(d)} = \frac{1}{3}(d/d\tau^2)$ and L_τ in equations (23) and (25) are independent on the density distribution throughout plasma cloud if the homogeneous atmosphere height of the density distribution is much less than the curvature radius of the plasma cloud layers. Thus the β-estimates, equations (19), (19a), and (27) are valid for any such density distribution.

3. EMISSION SPECTRUM

3.1. *Diffusion Regime* ($\tau_0 \gg 1$)

As we emphasized above, the X-ray spectrum of the upscattered low-frequency photons in plasma clouds is found as a result of solving of Comptonization stationary equation (CSE). The homogeneous CSE (15), i.e., with $\psi(x) = 0$ is transformed to

$$x^2N_1'' + x[x(1 + \epsilon) + 4]N_1' + (x^2\epsilon + 4x - \gamma)N_1 = 0. \tag{29}$$

Here $\epsilon = \mu'/\mu$ and $\mu = \eta(x\Theta, \Theta)/z^4$, (see eq. [4]), i.e.

$$\epsilon = \frac{\mu'}{\mu} = -\frac{(4.6 + 2.2x\Theta)\Theta}{1 + 4.6x\Theta + 1.1(x\Theta)^2}, \tag{30}$$

$$\gamma = \frac{\beta\lambda_{tr}}{\Theta\mu} \tag{31}$$

and

$$\gamma_0 = \frac{\beta}{\Theta[1 + f_0(\Theta)]}. \tag{32}$$

Because γ and ϵ depend weakly on the dimensionless energy x for $x < 2$, the solutions of equations (29) are expressed approximately by means of the Whittaker functions through the expression $Y_{\alpha,\beta}(x)$ which have convenient integral representation (see, e.g., Abramowitz & Stegan 1966). Thus

$$N_1(x) = x^{-2}\exp\left[-\frac{(1-\mu)x}{2}\right]Y_{2,\sqrt{9/4+\gamma}}[(1+\mu)x]. \tag{33}$$

In the case of low-frequency primary sources, i.e., $B_0(x, \tau) = \delta(x - x_0)r_1(\tau)$, with $x_0 \ll 1$, the spectrum of photon emerging from the plasma cloud is described by the simple formula

$$F_\nu(x, x_0) = \frac{\alpha_0(\alpha_0 + 3)}{2\alpha_0 + 3}\frac{1}{x_0}\left(\frac{x}{x_0}\right)^{3+\alpha_0} \quad \text{when} \quad 0 \le x \le x_0, \tag{34}$$

and

$$F_\nu(x, x_0) = \alpha_0(\alpha_0 + 3)\frac{e^{-x}}{x_0}\left(\frac{x}{x_0}\right)^{-\alpha_0}\frac{\int_0^\infty t^{\alpha-1}(x+t)^{\alpha+3}e^{-t}\,dt}{\Gamma(2\alpha+4)} \quad \text{where} \quad x_* > x \ge x_0. \tag{35}$$

Here $\Gamma(x)$ is the gamma function, $x_* = 0.5 + \gamma_0$ and

$$\alpha(x) = \sqrt{9/4 + \gamma(x)} - 3/2, \tag{36}$$

while

$$\alpha_0 = \sqrt{9/4 + \gamma_0} - 3/2. \tag{37}$$

The values of β are obtained by solving the equation $\beta = \beta(\tau_0)$ for given optical depth τ_0.

The solution of the Comptonization problem, equation (29) is characterized by a couple of asymptotic forms: the first one is low-frequency asymptotic form, $F_\nu \propto x^{-\alpha_0}$ when the dimensionless energy $x \ll \alpha_0$ and the second one is high-energy asymptotic form for $x \gg \alpha_0$ which is determined by Wien law $F_\nu \propto x^3e^{-x}$ in the nonrelativistic case. In order to find the spectrum $F(x, x_0)$ for high energies ($x > x_*$ and $x \gg \alpha_0$) in the relativistic case we present the occupation number $N_1(x)$ in a factorized form $N_1(x) = e^{-x}e^{-f(x)}$. Then N_1—equation (29)

reduces to Riccati's equation for $f(x)$:

$$x^2f'' + (4x - x^2)f' - x^2f'^2 = -\gamma_0[1 + 7.4\Theta q(\Theta)x + 13.54\Theta^2P(\Theta)x^2], \quad (38)$$

where $q(\Theta) = 1 - 0.42\Theta$ and $P(\Theta) = 1$–1.05. Deriving this equation from equation (29) we neglect ϵ-term with respect to 1 and the third and the fourth degree terms of z ($z = \Theta x$) in γ-polynomial with respect to quadratic polynomial of z. The solution of equation (38) can be represented by the following asymptotic series

$$f(x) = b_0 x + b_1 \ln x - \sum_{n=2}^{\infty} \frac{b_n}{(n-1)x^{n-1}}, \quad (39)$$

with coefficients b_n given by

$$b_0 = \frac{\sqrt{1 + 54.16\Theta^2P(\Theta)\gamma_0} - 1}{2}, \quad b_1 = \frac{4b_0 + 7.4\Theta q(\Theta)\gamma_0}{1 + 2b_0},$$

$$b_2 = \frac{3b_1 - b_1^2 + \gamma_0}{1 + 2b_0}, \quad (40)$$

and

$$b_{(2k-1)} = \frac{(6 - 2k)b_{2(k-1)} - 2\sum_{i=1}^{k-1} b_{(2k-1-i)}b_i}{1 + 2b_0},$$

$$b_{2k} = \frac{(5 - 2k)b_{(2k-1)} - b_k^2 - \sum_{i=1}^{k-1} b_{(2k-i)}b_i}{1 + 2b_0}$$

$$\text{for } k = 2, 3, \ldots \quad (41)$$

Finally we obtain spectrum $F(x, x_0)$ for $x > x_*$ through the formula

$$F(x, x_0) = c_0 x^3 e^{-x-f(x)} = c_0 x^{3-b_1} e^{-x(1+b_0)} \exp \sum_{n=2}^{\infty} \frac{b_n}{(n-1)x^{n-1}} \simeq c_0 x^{3-b_1} e^{-x(1+b_0)}. \quad (42)$$

The coefficient c_0 is determined by the continuity between the two parts of the spectrum (eq. [35] and eq. [42]) at $x \simeq x_*$. It is worthwhile noting the difference between the hard nonrelativistic and relativistic tail. Instead of a Wien tail, x^3e^{-x}, in the nonrelativistic case, in the relativistic case we have the steeper tail $x^{3-b_1}e^{-x(1+b_0)}$.

The spectra resulting from the Comptonization of soft photon radiation with $h\nu_0 = 10^{-3}kT_e$ in high-temperature plasma clouds for various values of kT_e and the parameter β are obtained by numerically solving equation (15), (or eq. [29]). A comparison of these solutions with the nonrelativistic models of ST80 are presented in Figure 2. It is seen that the nonrelativistic spectra are satisfactory for temperatures $kT_e <$ 30 keV and energies $h\nu < 50$ keV with optical depth of plasma cloud $\tau_0 > 2$. There is also shown in Figure 2 comparison between the analytical approximation of equations (34), (35), and (42) and the exact numerical solution of equation (29). Figure 2 shows that the new analytical formula works even much better than the modified nonrelativistic approximation of ST80 and fits excellent the numerical solution of equation (29) in the whole temperature range up to 100 keV. The modified nonrelativistic approximation of ST80 is determined by equations (34)–(37) with $x_* = \infty$ and $\gamma = \gamma_0$ (the latter is defined by eq.[32]). In order to test the accuracy of the numerical solution of equation (29) a couple of nonrelativistic solutions are shown in Figure 2. These include the modified ST80 formula for the monochromatic soft photon radiation $h\nu_0$ and the numerical solution of equation (29) with $\epsilon = 0$ and $\gamma = \gamma_0$ when the soft radiation is described by a blackbody with temperature $kT_0 = h\nu_0/2.7$.

3.2. *Optically Thin Case* ($\tau_0 < 2$)

In the case of small optical depths $\tau_0 < 2$ and high temperature $kT_e > 100$ keV the radiation field of photons which undergo repeated scattering form the specific angular distribution. ST85 discuss details of the angular distribution and polarization of photons escaping from optically thin layers. Here ϑ refers to the angle between the normal to the disk plane and a given direction and $\xi = \cos\vartheta$. The main features of the distribution are as follows: (i) The intensity increases monotonically from $\xi = 1$ to $\xi = 0$. (ii) The radiation flux as product of ξ and intensity I in given direction has its maximum at $\xi_{max} = (\tau/2)^{1/3} \ll 1$. (iii) It is mainly photons with $\xi_{eff} \approx \tau_0 \ln(1/2\tau_0)$ that stay in optically thin disk. Radiation from the optical disk generates a knife beam, it escapes from the disk at angles close to the disk plane.

Thus we can formulate the problem of the determination of the energy diffusion coefficient of Fokker–Plank equation in the case the knife beam radiation field. In appendix B we present the solution of the problem. In that approximation the photons gain energy in the course of random walk when they scatter in the backward directions. The asymptotic form of the energy diffusion coefficient $\eta(z, \Theta)$ at energies $h\nu \ll kT_e$ is found through the expression

$$\eta(z, \Theta) \simeq z^4 \frac{1 + (19/8)\Theta + \cdots}{1 + (15/8)\Theta + \cdots}. \quad (43)$$

Note that such relative weak temperature dependence of $\eta(z, \Theta)$ is explained by weakening of the Klein–Nishina differential cross section in the backward directions with increasing plasma temperature. The transport coefficient λ_{tr} (see eq. [1]) becomes smaller and it is almost constant, 1 for the whole high-energy range. In the spherical geometry the preferential directions of radiation propagation are concentrated along radial directions. The fraction of photons $H(\xi_*, 1)$ which escape between $\xi = \xi_*$ and $\xi = 1$ equals to $H(\xi_*, 1) = 1 - \xi_*^3 - 0.75\tau_0(1 - \xi_*^4)$. Here ξ refers to the cosine of angle between the radial direction and a given direction. The last relation shows the fraction of photons leaving plasma cloud and detained (because of scattering) at the directions with $\xi < \xi_*$ decline as ξ_*^3 and ξ_*^4, respectively.

The analytical approximation (34) and (35) fits successfully Monte Carlo calculations (Titarchuk & Hua 1994; Pozdnyakov et al. 1983; Zdziarski 1986) and γ and γ_0 used in the computations of α and α_0 (eqs. [36] and [37]) could be replaced by the following expressions

$$\gamma = \gamma_0(1 + 4.6z + 1.1z^2) \quad \text{and} \quad \gamma_0 = \frac{\beta[1 + (15/8)\Theta]}{\Theta[1 + (19/8)\Theta]}, \quad (44)$$

i.e., the temperature dependence of the space diffusion coefficient η_v can be replaced by that weak temperature dependence which follows from equation (43). The equation (35) is computed for all dimensionless energies $x > x_0$, i.e., $x_* = \infty$. The results are given in Figure 3 for the plasma temperatures $kT_e = 100$, 500 keV and for the plasma optical depths $\tau_0 =$ 0.1–2.

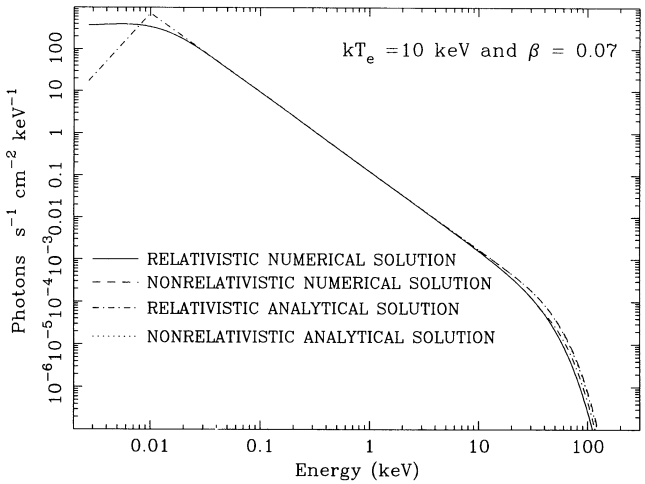

FIG. 2*a*

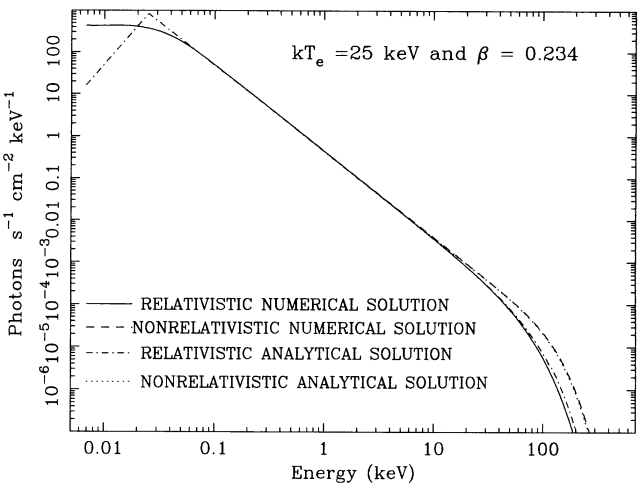

FIG. 2*b*

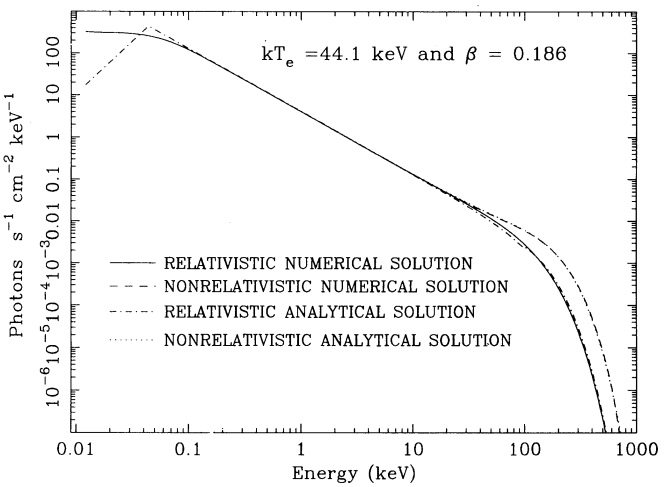

FIG. 2*c*

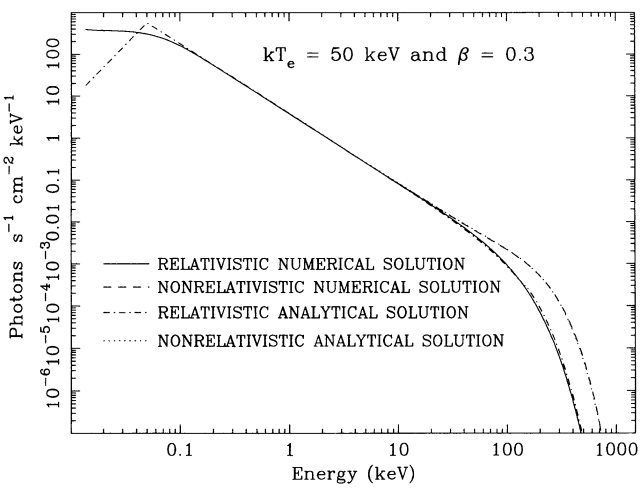

FIG. 2*d*

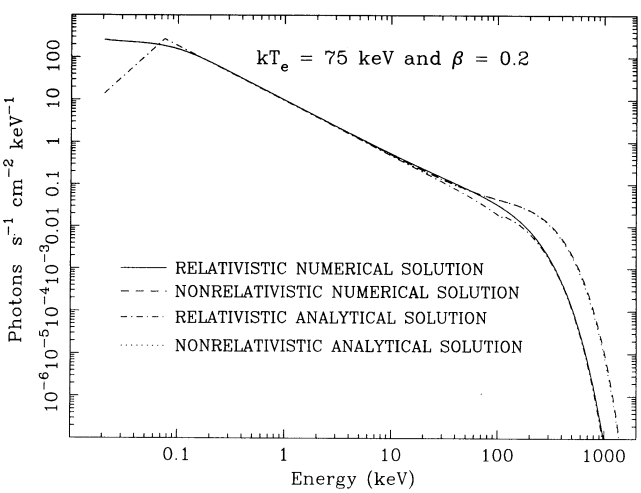

FIG. 2*e*

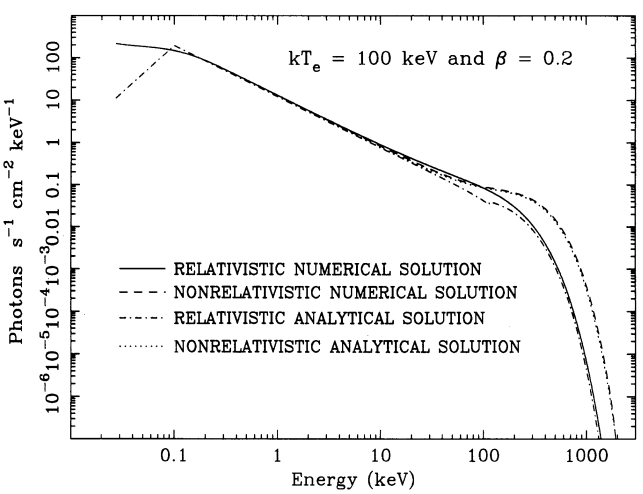

FIG. 2*f*

FIG. 2.—(*a*) Comparison of the outgoing photon spectra for plasma cloud with electron temperature $kT_e = 10$ keV for the modified nonrelativistic Comptonization model ST80 (eqs. [34]–[37] with $x_* = \infty$ and $\gamma = \gamma_0$, the latter is defined by eq. [32]) and the outgoing spectra calculated with relativistic corrections (eqs. [29], [34], [35], and [42]). (*b*) Same as (*a*) for $kT_e = 25$ keV. (*c*) Same as (*a*) for $kT_e = 44.1$ keV. (*d*) Same as (*a*) for $kT_e = 50$ keV. (*e*) Same as (*a*) for $kT_e = 75$ keV. (*f*) Same as (*a*) for $kT_e = 100$ keV.

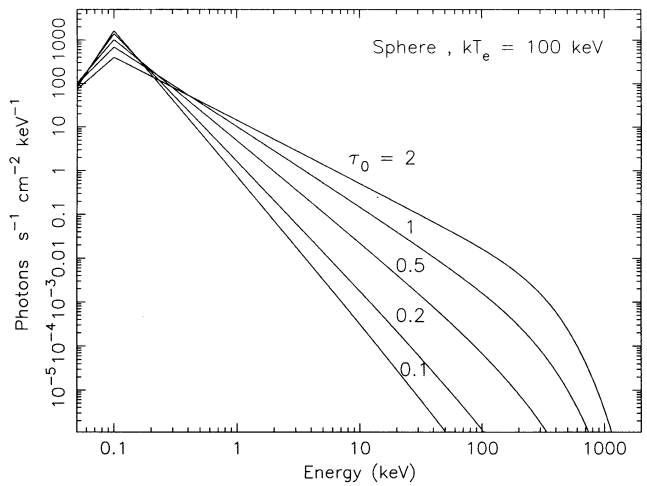

FIG. 3a

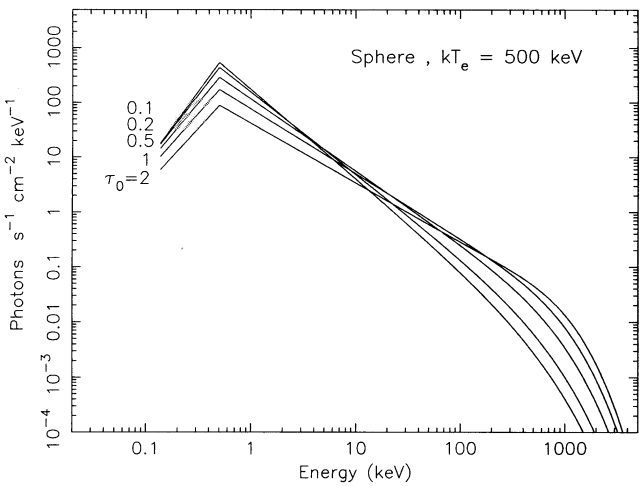

FIG. 3b

FIG. 3.—(*a*) Outgoing photon spectra for plasma cloud electron temperature $kT_e = 100$ keV in the optical thin case with optical depths in spherical geometry $\tau_0 = 0.1$–2 calculated with relativistic corrections (eqs. [35] and [44]). (*b*) Same as (*a*) for $kT_e = 500$ keV.

In the conclusion of this section we want to summarize two things: (i) The analytical and numerical relativistic solutions of equations (15) and (29) are much better than ST80 and they approximate quite well the Monte Carlo results (Titarchuk & Hua 1994) for $\beta < 0.6$–0.7, i.e., for the optical depth in spherical geometry more than 1 and for the optical depth in disk geometry more than 0.5 and for the temperature range up to 150 keV. It is important to point out that the diffusion coefficient $\eta(z, \theta)$ of the kinetic equations (6) (or eqs. [15] and [29]) should be replaced by the exact solution of Prasad et al. (1988) instead of using the formula (4) for $kT_e > 100$ keV. (ii) In the case of relative small optical depth $\beta > 0.4$ (the optical depth in spherical geometry $\tau_0 < 2$ and the optical depth in disk geometry $\tau_0 < 1$) and high temperatures up to 500 keV the analytical approximation (35) along with the appropriate corrections for the parameters γ and γ_0 (eq. [44]) works fairly well (Titarchuk & Hua 1994) and could be used as a model in data analysis.

Below we show how this analytical approach is applied for interpretation Cyg X-1 data.

4. SOURCE OF LOW-FREQUENCY PHOTONS

Sunyaev & Titatchuk (1989) (see also Paczynski 1978; Ionson & Kuperus 1984) formulated the problem of the interaction of radiation between hot and cold material in the framework of a sandwich model. Later this problem was also considered by Haardt & Maraschi (1991) with application to AGNs, and by Haardt et al. (1993) for the interpretation of OSSE observations of Cyg X-1. We shall present the detailed theory, numerical calculation and astrophysical applications of this model in a forthcoming paper (Titarchuk 1994). Here we will only present some very simple estimations which directly follows from the presence of a hot region in the vicinity of relatively cold material. As an example of a cold material we can consider an accretion disk with a surrounding hot corona or some part of a neutron star surrounded by a hot boundary layer.

We assume that the low-frequency photons are produced in the lower cold layers due to heating of cold material by the hard photons emerging from the hot region. Some fraction of the luminosity L irradiated outside therefore is deposited in the cold material because of the recoil effect on cold electrons and photoelectric absorption. The first process is more important for high-temperature regions with $kT_e \geq 20$ keV, as may be observed for Cyg X-1 (see, e.g., Sunyaev & Trümper 1979; ST80; Frontera & Dal Fiume 1992; Grabelsky et al. 1993) and for NGC 4151 (Maisack et al. 1993). The second process (i.e., photoabsorption) mainly defines the soft photon production in the cloud layers of the accretion disks in galactic sources when the temperature of the hot region is around a few keV (see, e.g., White, Stella, & Parmar 1988).

For simplicity we will consider only the recoil effect as the main source of the energy deposition in the cold material. This deposition flux, which equals the soft photon energy flux L_0, is determined by the expression

$$L_0 = \frac{(1 - A)L}{2} . \tag{45}$$

Here A is the albedo of the cold material, illuminated by the hard photon flux incident from the hot region. The formula for albedo can be obtained if we assume that the incident radiation spectrum F_ν has the specific upscattered shape given by equation (23) in ST80 and if we use the formula for the monochromatic albedo (Titarchuk 1987)

$$1 - A_\nu = \sqrt{\frac{\pi}{3}\frac{h\nu}{m_e c^2}} .$$

Then we can write

$$1 - A = \frac{\int_0^\infty (1 - A_\nu) F_\nu d\nu}{\int_0^\infty F_\nu d\nu} = \sqrt{\frac{\pi}{3}\frac{kT_e}{m_e c^2}}\,\frac{\Gamma(3/2 - \alpha)\Gamma(\alpha + 4.5)}{\Gamma(3/2)\Gamma(\alpha + 4)\Gamma(1 - \alpha)} . \tag{46}$$

To derive this formula we have used the method of integration presented in chapter 7.3 of ST85, assuming a spectral index $\alpha < 1$. The case $\alpha < 1$ contains the solution set of $x_0 \ll 1$ for recoil effect deposition. Another relationship between L and L_0 follows from the equation for the enhancement factor $d(a)$ due to upscattering of photons (ST80; ST85)

$$\frac{L}{L_0} = d(\alpha) x_0^{\alpha - 1} = \frac{\alpha(\alpha + 3)\Gamma(\alpha + 4)\Gamma(\alpha)\Gamma(1 - \alpha)}{\Gamma(2\alpha + 4)} x_0^{\alpha - 1} . \tag{47}$$

Excluding the ratio (L/L_0) in the system of equations (45) and (47) and using equation (46) we derive explicit equation for x_0

$$x_0 = \left[\frac{1}{2}\sqrt{\frac{\pi kT_e}{3m_e c^2}}\,\frac{\Gamma(3/2-\alpha)\Gamma(\alpha+4.5)\Gamma(\alpha)\alpha(\alpha+3)}{\Gamma(3/2)\Gamma(2\alpha+4)}\right]^{1/(1-\alpha)}. \tag{48}$$

The values of x_0 have to satisfy two conditions, namely $x_0 \ll 1$ and $1 - A \ll 1$. In Figure 4 the values of x_0 are plotted versus α for various plasma temperatures. For smaller kT_e, the set of the admissible α is shifted to smaller values and the left boundary of this range is determined by the evident inequality $x_0(\alpha) < \frac{1}{2}$.

For example in the case of Cyg X-1 (see below and also Haardt et al. 1993) $kT_e \simeq 150$ keV and the relevant α obey the condition $\alpha > 0.5$. From the right side the spectral slopes are limited by the equality $\alpha = 1$ because in this case the enhancement factor (ST80) is

$$\frac{L}{L_0} = \frac{4}{5}\ln\frac{1}{x_0} \tag{49}$$

but on the other hand (see eq. [45])

$$\frac{L}{L_0} = \frac{2}{1-A} = \frac{\Gamma(6)}{\Gamma(5.5)}\sqrt{\frac{3m_e c^2}{\pi kT_e}}\,\frac{4}{5}\ln\frac{1}{x_0}. \tag{50}$$

Comparing these equations we obtain that L/L_0 as determined by equation (50) exceeds (L/L_0) derived from equation (49) because

$$\frac{\Gamma(6)}{\Gamma(5.5)}\sqrt{\frac{3m_e c^2}{\pi kT_e}} > 1.$$

In other words, the deposition energy due to recoil effect in cold layer is so small that the produced soft photon radiation L_0 cannot be upscattered to the output radiation L because of the values of Comptonization parameter $y \simeq 12/\gamma \leq 3$ too small.

Taking into account free-free absorption for the albedo calculation we assume that more energy could be deposited in the cold material and consequently we shift these estimations to larger values of α (and thus to smaller values of y).

For given values of α, x_0, and luminosity L, we are able to estimate the size of the soft photon emission area S, using equation (47)

$$S = \left(\frac{2.7kT_0}{kT_e}\right)^{1-\alpha}\frac{L}{d(\alpha)\sigma T_0^4}. \tag{51}$$

Now we derive the equations for the enhancement factor L/L_0, the energy of the soft photons x_0 and the size of the soft photon emission area S with an assumption of the spectral shape of the relativistic upscattering hard tail of equation (42). Thus for the flux averaged albedo we can write

$$1 - A = \frac{\int_0^\infty (1-A_\nu)F_\nu\,d\nu}{\int_0^\infty F_\nu\,d\nu} \simeq \sqrt{\frac{\pi}{3}\frac{kT_e}{m_e c^2}}\,\frac{\Gamma(\delta+3/2)}{d^{0.5}\Gamma(\delta+1)}. \tag{52}$$

Here $F_\nu \simeq c_0 x^\delta e^{-xd}$, (see eq. [42]) and hence $d = 1 + b_0$ and $\delta = 3 - b_0$. In addition to equation (45), L and L_0 ($L_0 = 1$ in eqs. [34] and [35]) are related by the expression for the enhancement factor due to the upscattering of photons

$$\frac{L}{L_0} = \int_0^\infty F_\nu\,dx \simeq c_0\,\frac{\Gamma(\delta+1)}{d^{\delta+1}}. \tag{53}$$

As we have mentioned before the coefficient c_0 is determined by the continuity condition between the two parts of the spectrum (eqs. [35] and [42]) at $x \simeq x_*$:

$$c_0 \simeq \frac{\alpha_0(\alpha_0+3)e^{-b_0 x_*}}{(2\alpha_0+3)x_*^{\alpha_0+\delta}}\,x_0^{\alpha_0-1}. \tag{54}$$

Eliminating L and L_0 from the equations (42) and (53) and using the equation (52) we find at once the frequency of soft radiation

$$x_0 = \left[\frac{1}{2}\sqrt{\frac{\pi kT_e}{3m_e c^2}}\,\frac{e^{-b_0 x_*}\Gamma(\delta+3/2)\alpha_0(\alpha_0+3)}{x_*^{\alpha_0+\delta}d^{\delta+3/2}(2\alpha_0+3)}\right]^{1/(1-\alpha_0)}. \tag{55}$$

Therefore, by knowing the parameter β and the temperature kT_e and using equations (45) and (52) one can calculate the temperature of the soft photons

$$kT_0 = \frac{x_0 kT_e}{2.7}$$

and the size of the photon emission area S:

$$S = \pi R^2 \simeq \frac{1}{2}\sqrt{\frac{\pi}{3}\frac{kT_e}{m_e c^2}}\,\frac{\Gamma(\delta+3/2)}{d^{0.5}\Gamma(\delta+1)}\,\frac{L}{\sigma T_0^4}. \tag{56}$$

Equations (55) and (56) (also eqs. [45] and [51]) hold provided that $x_0 \ll 1$ and $\alpha_0 < 1$.

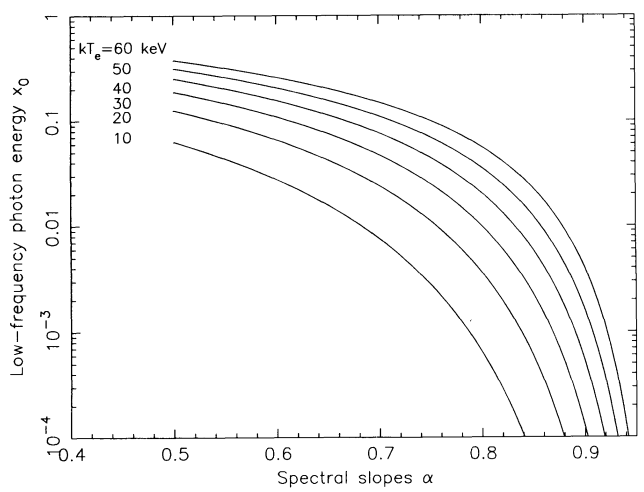

FIG. 4.—Set of x_0 vs. α is presented as a function of plasma temperature kT_e.

5. ASTROPHYSICAL APPLICATIONS

Now we illustrate briefly the relevance of the above model to current high-energy observations by OSSE and *GRANAT*. A more detailed analysis of the relevant data will be presented elsewhere (Titarchuk & Mastichiadis 1994).

5.1. *Cyg X-1*

There is a number of models to explain the hard radiation of Cyg X-1 (see, e.g., the review by Liang & Nolan 1984). One of the most popular is the Comptonization model according to which low frequency photons upscatter on hot electrons, thus producing the observed hard spectrum. The solutions obtained in § 3 allow one to estimate the characteristics of the hard photon emission region, the electron temperature, the optical

depth and the size of the upper hot layer, and also to determine the soft photon energy produced in cold layers of the accretion disk situated below the hot region.

The shape of the emission spectrum emerging from the plasma cloud is described by equations (35), (44) and depends only on two parameters β, and the value of the temperature kT_e.

Figure 5 shows the data obtained by the *EXOSAT*, *GRANAT*, and OSSE observations of Cyg X-1 (for details on the data see Done et al. 1992, Salotti et al. 1992, and Grabelsky et al. 1993). These are compared with calculations made by Haardt et al. (1993) for the ST80 model with $kT_e = 63$ keV, and $\tau_d = 2$ and by Haardt & Maraschi (1991), using a Monte Carlo sandwich model with $kT_e = 153$ keV and $\tau_d = 0.3$. Also shown are the analytical results obtained from equations (35), (44) with $kT_e = 153$ keV and $\beta = 1.02$ and all the parameter values kT_e, β correspond to the best-fit values. The above value of β corresponds to the half-thickness of the disk $\tau_0 = 0.15$ ($\tau_0 = \tau_d/2$); for spherical case it corresponds to $\tau_s = 0.62$. The comparison of the analytical best-fit with Zdziarski's analytical approximation (Zdziarski 1986) with $kT_e = 153$ keV and $\tau_s = 0.62$ is also given in Figure 5. None of these fits don't show the discrepancy between the theoretical curve and the data in energies less than 30 keV presented by Haardt et al. (1993) which they try to explain in terms of the reflection model, i.e., that the gap might be filled in by photons reflected from the underlying cold matter of the accretion disk.

Equations (48) and (51) can be used to estimate the energy of the soft photons $h\nu_0$ as well as the emission region area S. As

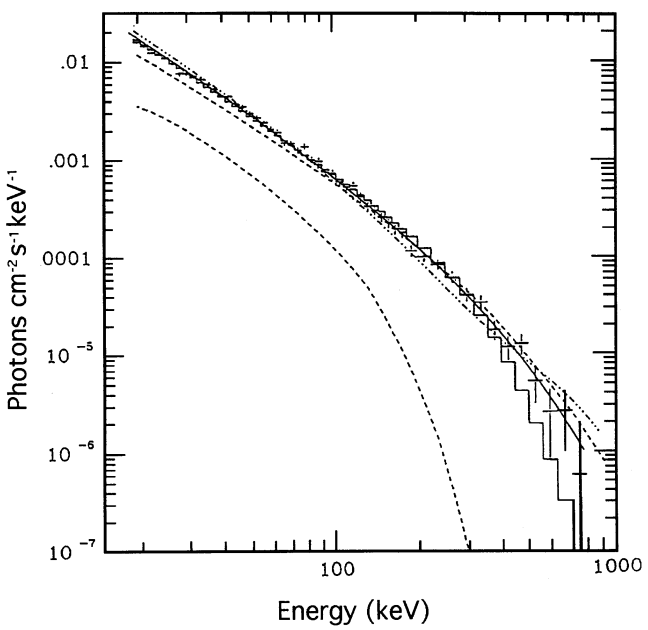

FIG. 5.—Data obtained during *EXOSAT*, *GRANAT*, and OSSE observation of Cyg X-1 (Done et al. 1992; Salotti et al. 1992; Grabelsky et al. 1993). These are compared with calculations made by Haardt et al. (1993) for ST80 model with $kT_e = 63$ keV and $\tau_d = 2$ (*histogram*) and by Haardt & Maraschi (1991) for a Monte Carlo sandwich model with $kT_e = 153$ keV, and $\tau_d = 0.3$ (*dashed line*) also with analytical results obtained with eqs. (35) and (44) (*solid line*), with $kT_e = 150$ keV and $\beta = 1.02$, which corresponds to the half-optical thickness of the disk $\tau_0 = 0.15$ ($\tau_0 = \tau_d/2$) or $\tau_s = 0.62$ in spherical geometry. The dash-dot-dot-dot line presents the Zdziarski (1986) analytical approximation for the given parameters $kT_e = 153$ keV and $\tau_s = 0.62$. All parameter values kT_e, τ, β correspond to the best-fit values.

long as these equations are obtained with the approximation of the ST80 model (i.e., without relativistic corrections), we use the best-fit parameters of ST80 for such estimations: the spectral slope $\alpha = 0.9$ and $kT_e = 75$ keV. The temperature value corresponds to the upper fit value and differs by 20% from the best values. We choose this temperature in order to fill the gap between the data and the theoretical model points in the hard energy region $E > 300$ keV.

Then the blackbody temperature of soft photons of 110 eV obtained from equation (48), implies an area $S = 10^{15}$ cm^2 or a radius of the emission region of ~ 14 Schwarzschild radii, which for a Cyg X-1 luminosity equals to 10^{37} ergs s^{-1} and mass of to 10 solar masses.

5.2. *NGC 4151*

The recent OSSE observations of Seyfert 1, NGC 4151 (Maisack et al. 1993) represent the most sensitive observations of this object in the energy range from 60 keV up to 1 MeV. The emission spectrum of NGC 4151 is supposed to be the typical Comptonization spectrum formed due to upscattering of ultraviolet radiation reproduced in the cold material of accretion disk (see, e.g., Dermer, Liang, & Canfield 1991). Zdziarski et al. (1993a) show that the OSSE (Maisack et al. 1993) and the *Ginga* (Yaqoob et al. 1993) observations of NGC 4151 are well explained by a nonthermal model with acceleration of relativistic electrons at an efficiency of less than 50% and with the remaining power dissipated thermally in the source. They point out that the pure thermal model gives a worse fit to the data than their hybrid nonthermal/thermal model.

On our part we want to emphasize that using the exact Comptonization solution with relativistic correction (eqs. [35] and [42]) for thermal model produces extremely good fit for the *Ginga* and the OSSE data.

Figure 6 shows the OSSE data and the best fit given by equation (29) or formulae (35), (42) with a plasma temperature of 46^{+8}_{-2} keV and Thomson optical depth of $1.1^{+0.2}_{-0.13}$ for the plane geometry and of $2.9^{+0.4}_{-0.3}$ for the spherical geometry (χ^2 probability = 0.1). The best fit with $kT_e = 46.3$ keV and $\beta = 0.21$ gives $\chi^2 = 11.4$ for 11 points and $\chi^2 = 12.2$ in the case of higher temperature 55 keV and $\beta = 0.32$.

Figure 7 shows the OSSE (Maisack et al. 1993) and the *Ginga* (Yaqoob et al. 1993) results and the best theoretical fit with a plasma temperature of 44^{+4}_{-4} keV and $\beta = 0.186^{+0.028}_{-0.023}$. The corresponding Thomson optical depths are 1.25 in disk geometry and 3.2 in spherical geometry. The best fit $kT_e = 44.1$ keV and $\beta = 0.186$ gives $\chi^2 = 33.03$ for twenty nine points and $\chi^2 = 35.4$ on the case of higher temperature 48.5 keV and $\beta = 0.214$. The absorber column density was kept fixed at the best-fit value given by Yaqoob et al. (1993), namely $N_h = 9.8 \times 10^{22}$ cm^{-2}.

Assuming an X-ray luminosity equal to 10^{43} ergs s^{-1} and using equations (55) and (56) with the best-fit Comptonization parameters, $\beta = 0.186$ and the temperature $kT_e = 44.1$ keV (the relevant parameters α_0, b_0, b_1, d, δ are functions of β and kT_e, and are found to be 0.5, 0.14, 1.28, 1.72 respectively) we produce the appropriate values of the photon blackbody temperature and the emission surface size: $kT_e = 4.9$ eV ($h\nu_0 = 12$ eV) and $R = 4.8 \times 10^{12}$ cm.

Thus we see that the thermal model provides a very good fit to the high-energy spectrum of NGC 4151 and furthermore no significant nonthermal emission would be irradiated. Electron temperature of $\sim$40–50 keV for thermal fit would be consis-

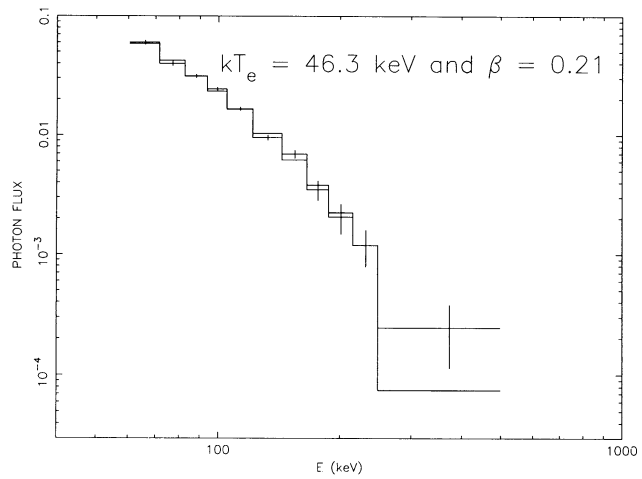

FIG. 6a

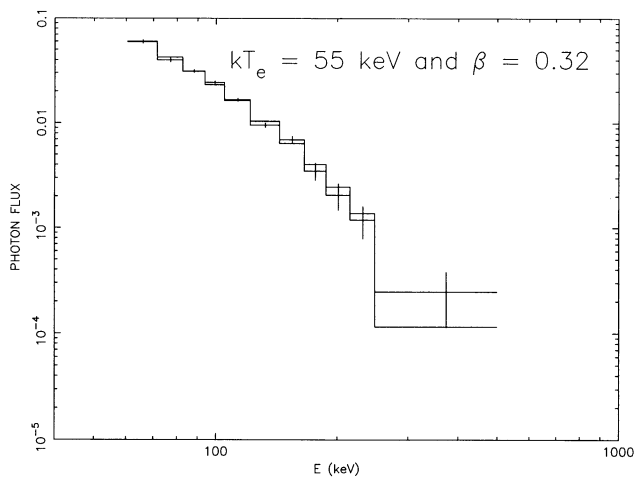

FIG. 6b

FIG. 6.—(*a*) OSSE data of NGC 4151 (Maisack et al. 1993) and the best fit by eq. (29) or formulae (35) and (42) with a plasma temperature of 46^{+8}_{-2} keV and Thomson optical depth of $1.1^{+0.2}_{-0.13}$ for the plane geometry and of $2.9^{+0.4}_{-0.3}$ for the spherical geometry (χ^2 probability = 0.1). The best fit with $kT_e = 46.3$ keV and $\beta = 0.21$ gives $\chi^2 = 11.4$ for 11 points. (*b*) Same as (*a*) in the case of plasma temperature 55 keV and $\beta = 0.32$ giving $\chi^2 = 12.2$.

tent with those which are predicted two-temperature accretion scenarios (e.g., Eilek & Kafatos 1983).

6. DISCUSSION AND CONCLUSION

The present description of high-energy spectra enables us to discuss several issues: the technique and main idea in getting Comptonization spectra; fits and explanation of observed X-ray spectra by the Comptonization models; constraints for physical parameters and geometry of compact objects; self-consistent determination of low-frequency radiation.

We display the theoretical spectra which result from Comptonization of low-frequency photons in plasma clouds. The problem is generalized in the case of subrelativistic energies and temperature and it is reduced to a Fokker–Plank technique even for very moderate plasma cloud optical depths. The main idea in getting the spectra is to present the emergent spectra as a convolution of the time development of the photon energy in the course of a photon's random walk in the plasma cloud, with the photon distribution over scatterings. The latter defines the probability for the photon to undergo a certain number of scatterings in the plasma cloud. The Comptonized X-ray spectrum is created by photons which suffer many more scatterings in plasma cloud than the average number (ST80; ST85). However, these photons produce the specific radiation field, with the specific angular and space distributions which are only determined by the plasma cloud optical depth and are independent of energy (ST85), i.e., photon random walk around plasma cloud occur independently on photon energy change (gain). Thus the upscattering spectral formation even in the case of small optical depths can be considered in terms of the Fokker–Plank approach when the photon energy change is weighted by the Compton scattering kernel (CSK) over photon directions and the photon scattering distribution. It turns out that, for high energies (much more than the average energy of the primary low-frequency photons), the main contribution to the above convolution integral comes from the exponential tail of the scattering distribution equation (17), which is the asymptotic form of any scattering distribution in a finite medium. Therefore, it is possible to derive a simple equation for the convolution determination, equation (15), the Comptonization stationary equation (CSE). The shape of the emergent spectrum is obtained as a solution of that equation. As a matter of fact, CSE contains only two parameters, the plasma temperature, kT_e, and the dimensionless escape rate, β, which control the spectral shape. The temperature or average energy of low-frequency photons determines simply the normalization of the spectrum. The solution of equation (15) (or eq. [29]) is presented in analytical form, equations (35)–(37) and (42) (eqs. [35] and [44] in the optical thin case, $\tau_0 < 2$). Numerical solutions are discussed as well (the Run method. Both of them are very convenient for spectral data analysis.

The shape of a number of X-ray spectra are fitted by the Comptonization model. We illustrate this in § 5. The spectral power-law slope along with the exponential cutoff contain information about the plasma optical depth and plasma temperature. The normalization of spectrum helps to determine the emission region surface area. This enables us to evaluate the energy flux per unit area, as long as the observed spectrum is fitted quite well by a Comptonized low-frequency blackbody spectrum (we obtain the parameters, optical depth and temperature, which give the Comptonization enhancement factor; see eqs. [47] and [53]). Furthermore, the assumption of a certain distance to the X-ray source, along with the count flux on Earth, give the emission region surface area.

The next question is how to distinguish between the two geometries (plane and spherical) by analyzing X-ray spectra. The optical depth values are obtained in a straight-forward calculation in the framework of a certain geometrical model (disk or sphere). However, a source characterized by very hard unsaturated Comptonization spectra, implies very high plasma temperatures and very small optical depths in the assumption of disk geometry. In this case, hard photons are mostly concentrated along the disk, forming a specific knife beam. Because of this, the possibility of observation of such hard photons from the disk drops when increasing the spectral hardness. Therefore, it is natural to suppose that hard photons come from quasi-spherical plasma clouds, rather than from the disk. Another possibility for determining the emission region geometry is through polarization measurements. For disk geometry, we would expect significant polarization with mag-

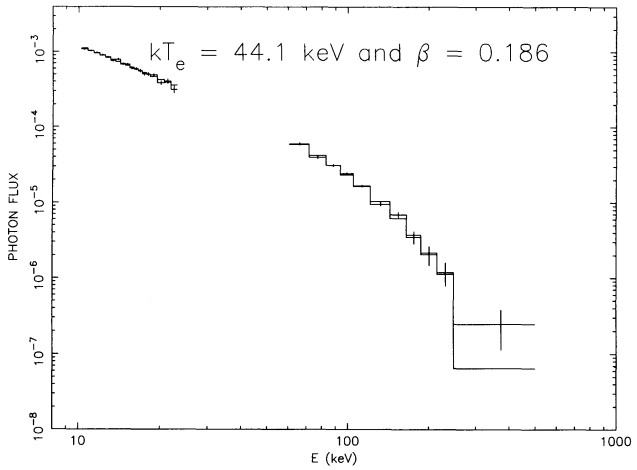

FIG. 7a

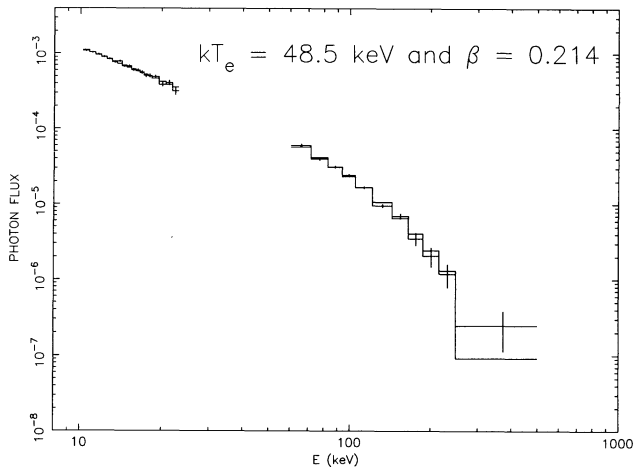

FIG. 7b

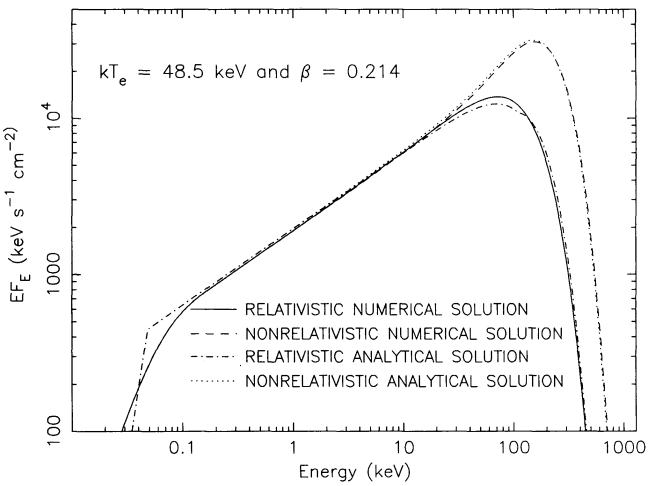

FIG. 7c

FIG. 7.—(*a*) OSSE (Maisack et al. 1993) and *Ginga* (Yaqoob et al. 1993) results for NGC 4151 and the best theoretical fit with a plasma temperature of 44^{+4}_{-4} keV and $\beta = 0.186^{+0.028}_{-0.023}$ and the appropriate Thomson optical depth are 1.25 in disk geometry and 3.2 in spherical geometry. The best fit with kT_e = 44.1 keV and $\beta = 0.186$ gives $\chi^2 = 33.03$ for 29 points. The absorber column density was kept fixed at the best-fit value given by Yaqoob et al. (1993), namely $N_h = 9.8 \times 10^{22}$ cm^{-2}. (*b*) Same as (*a*) for the case of plasma temperature of 48.5 keV and $\beta = 0.214$ giving $\chi^2 = 35.4$. (*c*) Dependence of EF_ν for the parameters kT_e and β the same as in Fig. 7*b*.

nitudes exceeding 40% in the case of optical depths less than 0.4 (ST85).

In § 4, we demonstrate that the self-consistent determination of the energy of low-frequency sources, which results from energy exchange between hot and cold material of an accretion disk, is possible only in the limited range of Comptonization parameters. If the Comptonization parameter is too big, $y > 6$ (or spectral indices $\alpha < 0.5$), a lot of energy is deposited due to the recoil effect in the cold layer, and the average energy of the photons escaping from the cold layer is comparable with the plasma temperature. In the opposite case of small Comptonization parameter values, $y < 3$ (or spectral indices $\alpha > 1$), the Comptonization spectrum suffers a shortage of hard photons. In that case, the deposition of energy due to the recoil effect in a cold layer is so small that the produced soft radiation cannot be upscattered to the output radiation.

I would like to acknowledge support from NRC grant. It is a pleasure to thank Nick White for his support and encouragement. The author would like to acknowledge extensive discussions with Demos Kazanas, Apostolos Matichiadis, Wan Chen, and John Contopoulos and also acknowledge N. Johnson, T. Yaqoob for the data sources. In particular the author thanks C. Dermer and A. Zdziarski and the anonymous referee who read this paper thoroughly and whose remarks and corrections help to improve the quality of this paper.

APPENDIX A

COMPTON RADIATIVE TRANSFER AND FOKKER–PLANK APPROXIMATION

At first we consider the case of plane geometry. However, in what follows there is no big difference between spherical and plane geometries. Therefore, a reader can repeat all the details for spherical geometry too.

Let us assume that we have a disk with Thomson optical half-thickness τ_0 filled by free electrons. The equation for the specific intensity, I of a radiation field is expressed through

$$\xi \frac{\partial I(\nu, \tau, \xi)}{\partial \tau} = B_0(\nu, \tau) + \frac{1}{n_e \sigma_T} \int_0^\infty d\nu' \int_{4\pi} d\Omega' \left[\frac{\nu}{\nu'} \sigma_s(\nu' \to \nu, \Omega' \cdot \Omega, T_e) I(\nu', \tau, \xi') - \sigma_s(\nu \to \nu', \Omega' \cdot \Omega, T_e) I(\nu, \tau, \xi) \right], \quad \text{(A1)}$$

where ν, ν' are the photon frequencies, τ is the Thomson optical coordinate with respect to the middle disk plane, Ω (incoming) and Ω' (outgoing) are photon directions, ξ (incoming) and ξ' (outgoing) are cosines of angles with respect to the disk normal. The intensity of radiation depends on the frequency, ν, the Thomson optical coordinate, τ, and the photon direction cosine, ξ. The

scattering kernel, σ_s (e.g., Pomraning 1973) depends on the plasma temperature T_e, the incoming (ν) and outcoming (ν') frequencies, and on the cosine of the angle between the two photon directions ($\zeta = \Omega' \cdot \Omega$). In order to reduce this equation to the equation for the zero moment of intensity, $J(\nu, \tau) = (1/4\pi) \int_{4\pi} d\Omega I$ over all solid angles, we multiply equation (A1) by $1/4\pi$ and then integrate over all solid angles Ω, keeping only zero moment of the intensity in the right-hand side:

$$\frac{\partial H(\nu, \tau)}{\partial \tau} = B_0(\nu, \tau) + \frac{1}{n_e \sigma_T} \int_0^\infty d\nu' \int_{4\pi} d\Omega' \left[\frac{\nu}{\nu'} S(\nu' \to \nu, T_e) J(\nu', \tau) - S(\nu \to \nu', T_e) J(\nu, \tau) \right] \tag{A2}$$

Here

$$S(\nu \to \nu', T_e) = \frac{1}{4\pi} \int_{4\pi} d\Omega' \sigma_s(\nu \to \nu', \Omega' \cdot \Omega, T_e)$$

and $4\pi H(\nu, \tau) = \int_{4\pi} d\Omega \xi I(\nu, \tau, \xi)$ is the specific flux of radiation at the frequency ν and at the optical coordinate τ.

The second equation which contains the first moment of intensity $H(\nu, \tau)$ is obtained by multiplying the original equation (A1) by $\xi/4\pi$ and then integrating. We keep two terms in the expansion of the intensity over ξ, $[I(\nu, \tau, \xi') = J(\nu, \tau) + 3H(\nu, \tau)\xi]$ in the first integral on the right-hand side of equation (A1). Introducing the second moment of intensity

$$K(\nu, \tau) = \frac{1}{4\pi} \int_{4\pi} d\Omega \xi^2 I(\nu, \tau, \xi) ,$$

and the transport function (see eq. [1]) we find

$$K(\nu, \tau) = -\frac{H(\nu, \tau)}{\lambda_{tr}(\nu, \Theta)} . \tag{A3}$$

Excluding the first moment of intensity, H in equations (A2) and (A3) and introducing the ratio of the second moment to the zero moment, $v = K/J$, the radiative transfer equation is expressed through

$$-\lambda_{tr}(\nu, \Theta) \frac{\partial}{\partial \tau} \frac{\partial [vJ(\nu, \tau)]}{\partial \tau} = B_0(\nu, \tau) + \frac{1}{n_e \sigma_T} \int_0^\infty d\nu' \int_{4\pi} d\Omega' \left[\frac{\nu}{\nu'} S(\nu' \to \nu, T_e) J(\nu', \tau) - S(\nu \to \nu', T_e) J(\nu, \tau) \right] . \tag{A4}$$

Here the differential operator

$$L_\tau = \frac{\partial}{\partial \tau} \left(\frac{\partial}{\partial \tau} v \right) \tag{A5}$$

on the left-hand side, and the appropriate energy integral operator L_ν on the right-hand side, act on the average intensity $J(\nu, \tau)$. Thus we can rewrite equation (A4) in the operator form

$$L_\nu J(\nu, \tau) + L_\tau J(\nu, \tau) = -\lambda_{tr}^{-1}(\nu, \Theta) B_0(\nu, \tau) . \tag{A6}$$

We have to add to equation (A6) the boundary condition which implies that photon scattering takes place only in the disk (the scattered photon flux from outside is zero); hence

$$4\pi H(\nu, \tau_0) = \int_0^{2\pi} d\varphi \int_0^1 \xi I(\nu, \tau_0, \xi) d\xi . \tag{A7}$$

Expressing H through K (eq. [A3]) and finally through J by means of the ratio v, we obtain the boundary condition at the edge of the disk, $\tau = \tau_0$:

$$\lambda_{tr} \frac{\partial [vJ(\nu, \tau_0)]}{\partial \tau} + v_0 J(\nu, \tau_0) = 0 . \tag{A8}$$

Here

$$v_0 = \frac{\int_0^1 \xi I(\nu, \tau_0, \xi) d\xi}{\int_0^1 I(\nu, \tau_0, \xi) d\xi} .$$

We need to note that ratios v and v_0, in general, depend on the frequency ν and the Thomson optical coordinate τ. However, in the cases of interest for Compton upscattering, the angular distribution of radiation field is determined by the plasma cloud optical depth τ_0, and is independent of the photon energy (ST85), $h\nu$ and hence, these ratios are functions of the optical coordinate τ only. For an isotropic ($\tau_0 \gg 1$) and almost collimated ($\tau_0 < 2$) radiation fields, these ratios are nearly constant. For an isotropic field, $v = \frac{1}{3}$ and $v_0 = \frac{1}{2}$. For the beam collimated near the direction for which cosine $\xi = \xi_*$, $v = \xi_*^2$ and $v_0 = \xi_*$. We should remind that, the beam cosine ξ_*, depends on τ_0 only, and is independent of the energy, $h\nu$ (ST85). Thus for the isotropic case, ($\tau_0 \gg 1$), the space operator L_τ is reduced to the operator

$$L_\tau^{(d)} = \frac{1}{3} \frac{d^2}{d\tau^2} \tag{A9}$$

with the boundary operator, l_τ

$$l_\tau = \lambda_{tr} \frac{\partial}{\partial \tau} + \frac{3}{2} . \tag{A10}$$

In the case of the beam field ($\tau_0 < 1$), because the form of L_τ, (eq. [A5]) is very sensitive to the exact determination of the cosine ξ_*, the space operator L_τ with the appropriate boundary condition can be represented in a more elegant way by the single integral operator, equation (23). Also, the diffusion operator L_τ^d is derived from the integral space equation (25) for the case $\tau_0 \gg 1$. In order to do this we expand the functon $B(\tau)$ of equation (25) in a Tayler series over $x = \tau' - \tau$, keeping only the three terms

$$B(\tau') = B(\tau) + B'(\tau)x + \frac{B''(\tau)}{2} x^2 . \tag{A11}$$

The zero, first and second momenta of the exponential integral $E_1(|\tau - \tau'|)$ over the range of τ', from $-\tau_0$ to τ_0 equal to 2, 0, 4/3, respectively. Using these values we find

$$\tfrac{1}{3} B''(\tau) = -B_0(\tau) . \tag{A12}$$

It is worthwhile noting that the accuracy of the representation of momenta for E_1 is of order of $\tau_0^2 e^{-\tau}$ for all $\tau \ll \tau_0 - 1$.

In § 2.1 we formulate the statement that the solution of equation (6) can be represented by the convolution from (8), if the right-hand side of equation (6) can be factorized in the form:

$$\Phi(\tau, v) = r(\tau)\psi(v) . \tag{A13}$$

This statement is general and is valid for any boundary problem of the equation (A6), i.e., if the left-hand side of arbitrary equation is a result of the action of the sum of two operators, L_τ and L_v and the right-hand side is factorized, as in equation (A13). The validity of the convolution form, Eq. (8) as the solution of equation (A6) (or eq. [6]) is checked by the following substitution:

$$\int_0^\infty R(\tau, u) L_v N(v, u) du + \int_0^\infty L_\tau R(\tau, u) N(v, u) du = -\psi(v) r(\tau) . \tag{A14}$$

Using equations (9)–(12) we find

$$\int_0^\infty R(\tau, u) \frac{\partial N(v, u)}{\partial u} du + \int_0^\infty \frac{\partial R(\tau, u)}{\partial u} N(v, u) du = \int_0^\infty \frac{\partial N(v, u) R(\tau, u)}{\partial u} du = -\psi(v) r(\tau) . \tag{A15}$$

The integral energy operator, L_v of equation (A6) was first reduced to the Fokker–Plank form by Kompaneets (1956) for the case of nonrelativistic photon energies and plasma temperatures. Subsequently, various authors have generalized Kompaneets' work up to the subrelativistic energies and temperatures (e.g., Cooper 1971; Prasad et al. 1988). In § 2.1 we present L_v in the Cooper–Prasad's form.

In order to develop the same approach for spherical geometry we need only to replace the plane space gradient of equation (A1) by the spherical space gradient:

$$\nabla I = \xi \frac{\partial I}{\partial \tau} + \frac{1 - \xi^2}{\tau} \frac{\partial I}{\partial \xi}$$

and to repeat the integration over all solid angles. Here ξ refers to the cosine of the angle between the photon direction and the radial direction.

APPENDIX B

DIFFUSION COEFFICIENT FOR THE COMPTON FOKKER-PLANK EQUATION IN THE COLLIMATED RADIATION FIELD

Prasad et al. (1988) have derived equation (3) for the energy diffusion coefficient η_v of the Fokker–Plank equation (6) (or eq. [A6]). The solution of equation (3) reads

$$\eta(z, \Theta) = \frac{1}{\Theta} \int_z^\infty dz' \exp\left[\frac{(z - z')}{\Theta}\right] \zeta(z', \Theta) . \tag{B1}$$

Here,

$$\zeta(z', \Theta) = \langle (z - z') \rangle = \int_0^\infty (z' - z) dS_c(z \to z', \Theta) . \tag{B2}$$

The weighted energy change $\zeta(z', \Theta)$ is presented by the integral (compare with Prasad et al. 1988)

$$\zeta(z', \Theta) = \int dv f(v) G \,, \tag{B3}$$

$$G = \frac{3/\lambda}{16\pi} \int_0^{2\pi} d\varphi \int_{-1}^{1} [\delta(\psi - \psi_+) + \delta(\psi - \psi_-)] d\psi \cdot (z - z') \left\{ 1 + \left[1 - \frac{1 - \xi}{\lambda^2 DD'} \right]^2 + \frac{(1 - \xi)^2 z z'}{\lambda^2 DD'} \right\} \delta\left(\xi - 1 + \lambda \frac{D}{z'} - \lambda \frac{D'}{z} \right) . \tag{B4}$$

In the case of a collimated radiation field by using Dirac delta function the integral over photon direction Ω' is reduced to the sum of two terms which correspond to the fixed photon direction $\vartheta_+ = \arccos \psi_+ \simeq 0$ and $\vartheta_- = \arccos \psi_- \simeq \pi$. The integral over z' is obtained by using the Dirac delta function which uniquely fixes the dimensionless photon energy z' in terms of z, the photon directions ϑ_+, ϑ_-, and the electron velocity v. In equations (B3) and (B4)

$$f(v) \equiv \frac{\lambda^5 \exp(-\lambda/\Theta)}{4\pi\Theta c^3 K_2(1/\Theta)} \tag{B5}$$

the relativistic Maxwellian distribution at electron temperature Θ, K_2 is the modified Bessel function of the second order, and

$$D \equiv 1 - \mu v/c \,, \qquad D' \equiv 1 - \mu' v/c \,, \qquad \lambda \equiv 1/\sqrt{1 - v^2/c^2} \,. \tag{B6}$$

Here, μ and μ' are the cosines of incoming (outgoing) photon directions and electron velocity direction respectively, ξ is the cosine of the angle between photon incoming and outgoing directions. In our case of a collimated radiation field we assume that $\xi \sim 1$ or $\xi \sim -1$. The Dirac delta function is used to fix z',

$$z' = \frac{zD}{D' + (1 - \xi) z/\lambda} \,. \tag{B7}$$

The term of equation (B4) which corresponds to the scatterings in the forward direction ($\xi = 0$) is eliminated, because $z - z' = 0$. Thus, integrating equation (B4) and taking into account equations (B5)–(B7) we obtain

$$\zeta(z', \Theta) = \frac{1}{2\Theta K_2(1/\Theta)} \int_1^{\infty} \lambda^2 \exp\left(-\frac{\lambda}{\Theta} \right) d\lambda \int_{x_-}^{x_+} G \, dx \,, \tag{B8}$$

Here

$$G(\lambda, z, x) = \frac{3}{2\lambda^2} \frac{z^3 (1 - x)}{(1 + x)^3} \left(x + \frac{z}{\lambda} \right) \left\{ \left[1 - \frac{1}{\lambda^2 (1 - x^2)} \right]^2 + \frac{1}{\lambda^4 (1 - x^2)^2} \right\} \tag{B9}$$

and

$$x = \mu \frac{v}{c} \,, \qquad x_{+(-)} = +(-) \frac{\sqrt{\lambda^2 - 1}}{\lambda} \,. \tag{B10}$$

Since we are interested in getting the power-law part of the spectrum, we take into account only the Doppler effect and we neglect the term $2z/\lambda$ of the function G which is responsible for the recoil effect. In order to get $\eta(z, \Theta)$ we integrate equation (B1), using equations (B8) and (B9)

$$\eta(z, \Theta) = \tfrac{3}{2} \{ [z^4 + 4\Theta P_3(z, \Theta)] I_1(\Theta) - 4 P_3(z, \Theta) I_2(\Theta) \} \,. \tag{B11}$$

Here

$$P_3(z, \Theta) = z^3 + 3\Theta z^2 + 6\Theta^2 z + 6\Theta^3 \,, \tag{B12}$$

$$I_1 = \frac{1}{\Theta K_2(1/\Theta)} \int_1^{\infty} e^{-\lambda/\Theta} F_1(\lambda) d\lambda \tag{B13}$$

and

$$I_2 = \frac{1}{\Theta K_2(1/\Theta)} \int_1^{\infty} e^{-\lambda/\Theta} F_2(\lambda) d\lambda \,. \tag{B14}$$

The functions $F_1(\lambda)$ and $F_2(\lambda)$ are expressed through elementary functions:

$$F_1(\lambda) = \frac{(\lambda^2 - 1)^{1/2}}{\lambda_2} \left(1 + \frac{28}{\lambda^2} \right) + \frac{3(\lambda^2 - 1)^{3/2}}{\lambda^4} + \frac{1}{\lambda^3} \left(10 + \frac{4}{\lambda^2} \right) \ln \frac{\lambda - (\lambda^2 - 1)^{1/2}}{\lambda + (\lambda^2 - 1)^{1/2}} \,, \tag{B15}$$

$$F_2(\lambda) = \frac{1}{3} \frac{(\lambda^2 - 1)^{3/2}}{\lambda^3} + \frac{3(\lambda^2 - 1)^{1/2}}{\lambda^3} + \frac{1}{\lambda^2} \left(1 + \frac{1}{2\lambda^2} \right) \ln \frac{\lambda - (\lambda^2 - 1)^{1/2}}{\lambda + (\lambda^2 - 1)^{1/2}} \,. \tag{B16}$$

Integration by part gives us

$$\Theta\int_1^\infty e^{-\lambda/\Theta}\frac{(\lambda^2-1)^{1/2}}{\lambda^2}\,d\lambda=\Theta\int_1^\infty e^{-\lambda/\Theta}\frac{(\lambda^2-1)^{3/2}}{\lambda^4}\,d\lambda+\frac{1}{3}\int_1^\infty e^{-\lambda/\Theta}\frac{(\lambda^2-1)^{3/2}}{\lambda^3}\,d\lambda\,, \tag{B17}$$

and thus, the energy diffusion coefficient $\eta(z,\Theta)$ is represented as follows

$$\eta(z,\Theta)=\tfrac{3}{2}\{z^4 I_1(\Theta)-4P_3(z,\Theta)R(\Theta)\}\,. \tag{B18}$$

It is easy to show by expanding $F_1(\lambda)$ and $F_2(\lambda)$ over x_+, (eqs. [B10], [B15], and [B16]) that

$$I_1(\Theta)=\frac{1+(19/8)\Theta\ldots}{1+(15/8)\Theta\ldots}\,, \tag{B19}$$

and that $R(\Theta)$ is of order Θ^2 [$R(\Theta)=O(\Theta^2)$]. It is worthwhile noting that the radiation field in a plasma cloud of small optical depth is never strongly collimated and the half-width of the beam is of order (15°–20°). Therefore, in order to apply equation (B18) in the realistic situation, we have to take into account the deviation of the cosine of scattering angle from -1 (in the preceding consideration we take into account only the scattering angle equals to π, because the zero angle gives rise to zero energy change). Using equation (B3), (B4) and (B7), we can show that the factor $c=3/2$ in equation (B18) should be replaced by the correct factor

$$c=\frac{3(1-\xi)(1+\xi^2)}{8} \tag{B20}$$

For a typical scattering angle cosine is ~ -0.8, this gives $c\simeq 1$.

REFERENCES

Abramowitz, M., & Stegan, I. 1966, Handbook of Mathematical Functions (Washington: NBS)
Apal'kov, Yu., et al. 1992, in Frontiers of X-ray Astronomy, ed. Y. Tanaka, K. Koyama, & H. Kunieda (Tokyo: Universal Acad. Press), 251
Brinkmann, W., Fabian, A. C., & Giovanelli, F. 1990, Physical Processes in Hot Cosmic Plasmas, NATO ASI Series (Dordrecht: Kluwer)
Chandrasekhar, S. 1960, Radiative Transfer (New York: Dover)
Chapline, G., & Stevens, J. 1973, ApJ, 184, 1041
Cooper, G. 1971, Phys. Rev. D, 3, 10, 2312
Dermer, C. D., Liang, E. P., & Canfield, E. 1991, ApJ, 369, 410
Done, C., Mulchaey, J. S., Mushotzky, R. F., & Arnaud, K. A. 1992, ApJ, 395, 275
Eilek, J. A., & Kafatos, M. 1983, ApJ, 271, 804
Frontera, F., & Dal Fiume, D. 1992, in Frontiers of X-ray Astronomy, ed. Y. Tanaka, K. Koyama, & H. Kunieda (Tokyo: Universal Acad. Press), 311
Grabelsky, D. A., et al. 1993, in Proc. First *Compton Observatory* Symp., ed. M. Friedlander, N. Gehrels, & D. J. Macomb (New York: AIP, 345
Grebenev, S. A., & Sunyaev, R. A. 1987, AZh Pis'ma, 13, 1042 (Soviet Astron. Lett. 1987, 13, 438)
Guessoum, N., & Kazanas, D. 1990, ApJ, 258, 525
Haardt, F., Done, C., Matt, G., & Fabian, A. C. 1993, ApJ, 411, L95
Haardt, F., & Maraschi, L. 1991, ApJ, 380, L51
Ionson, J. A., & Kuperus, M. 1984, ApJ, 284, 389
Kompaneets, A. S. 1956, Zh. Eksper, Teoret. Fiz., 31, 876 (Soviet. Phys.–JEPT, 4, 730 [1957])
Liang, E. P., & Nolan, P. L. 1984, Space Sci. Rev., 38, 353
Maisack, M., et al. 1993, ApJ, 407, L61
Paczynski, B. 1978, Acta Astron., 28, 241
Pozdnyakov, L. A., Sobol, I. M., & Sunyaev, R. A. 1983, Ap. Space Phys. Rev., 2, 189
Prasad, M. K., Shestakov, A. I., Kershaw, D. S., & Zimmerman, G. B. 1988, J. Quant. Spectrosc. Rad. Transf., 40, 29
Pomraning, G. 1973, Radiation Hydrodynamics (Oxford: Pergamon Press)
Solatti, L., et al. 1992, A&A, 253, 145
Shapiro, S., Lightman, A., & Eardley, D. 1976, ApJ, 204, 187
Shestakov, A. I., Kershaw, D. S., & Prasad, M. K. 1988, J. Quant. Spectrosc. Rad. Transf., 40, 577
Sunyaev, R. A., & Titrachuk, L. G. 1980, A&A, 86, 121 (ST80)
———. 1985, A&A, 143, 374 (ST85)
———. 1989, in Proc. 23d ESLAB Symp. on Two Topics in X-ray Astronomy, ed. N White (Noordwijk: ESA), 1, 627
Sunyaev, R. A., & Trümper, J. 1979, Nature, 279, 506
Titarchuk, L. G. 1987, Astrofizika, 26, 57 (Astrophysics. 1988, 26, 97)
———. 1988, Astrofizika, 29, 369 (Astrophysics. 1988, 29, 634)
———. 1994, in preparation
Titarchuk, L. G., & Hua, X. M. 1994, ApJ, in press
Titarchuk, L. G., & Mastichiadis, A. 1994, ApJ, 433, L33
White, N. E., Stella, L., & Parmar, A. N. 1988, ApJ, 324, 363
Yaqoob, T., et al. 1993, MNRAS, 262, 435
Zdziarski, A. A. 1986, ApJ, 303, 94
Zdziarski, A. A., Lightman, A. P., & Maciolek-Niedzwieski, A. 1993a, ApJ, 414, L93
Zdziarski, A. A., Zycki, P. T., Svensson, R., & Boldt, E. 1993b, ApJ, 405, 125